

**Design and evaluation of Quinazoline derivatives against
breast cancer by dual targeting of HDAC and EGFR
through *in-silico* modeling and screening *in-vivo* using
DMBA induced mammary carcinoma model**

**A Dissertation Submitted to
THE TAMIL NADU DR. M.G.R. MEDICAL UNIVERSITY
CHENNAI - 600032**

**In partial fulfillment of the requirements for the award of the Degree of
MASTER OF PHARMACY
IN
PHARMACOLOGY**

Submitted by

PAVITHRA.S

(Reg.No.261725812)

Under the guidance of

Dr.K.SURESH KUMAR, M.Pharm, Ph.D.,

Department of Pharmaceutical Chemistry



**KMCH COLLEGE OF PHARMACY
KOVAI ESTATE, KALAPPATTI ROAD
COIMBATORE - 641048**

NOVEMBER 2019

PROF. Dr. A. RAJASEKARAN, M. PHARM, Ph. D,

Principal,

KMCH College of Pharmacy,

Kovai Estate, Kalappatti Road,

Coimbatore - 641048

CERTIFICATE

This is to certify that the dissertation work entitled “**Design and evaluation of Quinazoline derivatives against breast cancer by dual targeting of HDAC and EGFR through *in-silico* modeling and screening *in-vivo* using DMBA induced mammary carcinoma model**” was carried out by **PAVITHRA.S (Reg No.261725812)**. The work mentioned in the dissertation was carried out at the Department of Pharmacology, KMCH College of Pharmacy, Coimbatore, Tamil Nadu, under the guidance of **Dr.K.SURESH KUMAR, M.Pharm, Ph.D.**, for the partial fulfilment for the Degree of Master of Pharmacy during the academic year 2018-2019.

Date:

Prof. Dr. A. RAJASEKARAN, M.Pharm., Ph.D.,

Place: Coimbatore

PRINCIPAL

Dr.K.SURESH KUMAR, M.Pharm, Ph.D.,

Professor, Head of the Department of Pharmaceutical Chemistry,

KMCH College of Pharmacy,

Kovai Estate, Kalapatti Road,

Coimbatore - 641048

CERTIFICATE

This is to certify that the research work entitled “**Design and evaluation of Quinazoline derivatives against breast cancer by dual targeting of HDAC and EGFR through *in-silico* modeling and screening *in-vivo* using DMBA induced mammary carcinoma model**” was carried out by **PAVITHRA.S (Reg No.261725812)**. The work mentioned in the dissertation was carried out at the Department of Pharmacology, KMCH College of Pharmacy, Coimbatore, Tamil Nadu, under my supervision and guidance for the partial fulfilment for the Degree of Master of Pharmacy during the academic year 2018-2019.

Date:

Place: Coimbatore

Dr.K.SURESH KUMAR, M.Pharm, Ph.D.,

DECLARATION

I hereby declare that the dissertation work entitled “**Design and evaluation of Quinazoline derivatives against breast cancer by dual targeting of HDAC and EGFR through *in-silico* modeling and screening *in-vivo* using DMBA induced mammary carcinoma model**” submitted to The Tamil Nadu Dr. M.G.R. Medical University, Chennai, in partial fulfillment for the Degree of **Master of Pharmacy in Pharmacology** was carried out under the guidance of **Dr.K.SURESH KUMAR**, M.Pharm, Ph.D., at the Department of Pharmacology, KMCH College of Pharmacy, Coimbatore, Tamil Nadu during the academic year 2018-2019.

This research work either in part or full does not constitute any of other thesis / dissertation.

Date:

Place: Coimbatore

PAVITHRA.S (Reg No.261725812).

EVALUATION CERTIFICATE

This is to certify that the research work entitled “**Design and evaluation of Quinazoline derivatives against breast cancer by dual targeting of HDAC and EGFR through *in-silico* modeling and screening *in-vivo* using DMBA induced mammary carcinoma model**” submitted by **PAVITHRA.S (Reg No.261725812)** to the Tamil Nadu Dr. M.G.R. Medical University, Chennai, in the partial fulfilment for the Degree of **Master of Pharmacy in Phamacology**, is a bonafide work carried out by the candidate at KMCH College of Pharmacy, Coimbatore, Tamil Nadu during the academic year 2018-2019 and the same was evaluated.

Examination Centre: KMCH College of Pharmacy, Coimbatore

Date:

Internal Examiner

External Examiner

Convener of Examination

ACKNOWLEDGEMENT

This dissertation entitled” **“Design and evaluation of Quinazoline derivatives against breast cancer by dual targeting of HDAC and EGFR through *in-silico* modeling and screening *in-vivo* using DMBA induced mammary carcinoma model”** would not have been a possible one without the grace of god almighty and effort of my dear friends who gave me moral support till the completion of my project.

First and foremost I express my gratitude to my esteemed guide, **Dr.K.Suresh Kumar, M.Pharm, PhD.**, Professor, Department of Pharmaceutical Chemistry, KMCH College of Pharmacy, Coimbatore, for his guidance, advice, and his hope on me and his effort for the successful completion of this work.

I express my sincere thanks to **Dr. G. Ariharasivakumar, M.Pharm, Ph.D., Professor and HOD, Department of Pharmacology** for guiding me and helping me throughout. I will forever be grateful for his invaluable ideas and support.

I am extremely grateful to my **parents** for their love and constant support in all the situations. Also, I express my thanks to my friends for their support and valuable prayers and timely help.

With great pleasure I wish to place my indebtedness to Principal **Dr. A. Rajasekaran M.Pharm.Ph.D**, for his support and for giving me an opportunity to do my project work.

My respectful regards to our beloved chairman **Dr. Nalla G.Palanisamy** and our respected Managing trustee, **Dr. Thavamani D. Palanisamy**, KMCH College of Pharmacy, Coimbatore.

I express my deep gratitude to my teachers **Dr.N.Adhirajan, M.pharm, Ph.D., Mr.I.Ponnilarasan, Dr.T.Sengottuvel, Mrs.Abarnadevika, Dr.Hurmath Unnisha, Mrs.Vennila, Dr.Tamilselvi, Mrs.SathyaPrabha, Dr.K.K.Sivakumar, Dr.Sundaramoorthy, etc.**, for their immense support, help and suggestions. I express my

sincere thanks to all my teachers who moulded me and guided me throughout.

I am much indebted to my lovable friends **Kavitha, Athira and Vishali** who stood on behalf of me in various situations. Their dedication, love and support had helped me a lot especially during my hard time. I am grateful and indebted for their help throughout.

I take this opportunity to extend my indebtedness thanks to my friends, **Rajkumar, Rajesh, Gopalsatheeshkumar, Satheesh, Jayanthi, Karthikaa, Malathi, Nijanthan, Suresh Kumar, Siva Kumar** for their contributions directly and indirectly during this period.

I especially convey my gratitude and indebtedness to **Mr.Vinoth, Mr.Ganesh Kumar** who helped and supported me in finishing my project work in various aspects.

Our special thanks to **IIT Madras** for their timely help for the analytical studies. I express my thanks to lab technicians **Mr. Siva, Mrs. Akila, Mrs. Selvi, Mr. Tamilarasan, Ms. Sridevi, Ms. Jeeva, Mrs. Sudha, Mrs. Thenmozhi, Mr. Saravanan, Mrs. Menaga.**

I am grateful to **Mrs. Dhanalakshmi** for helping in animal maintenance during the study.

Finally, my thanks go to all the people who have supported me to complete the research work directly or indirectly.

PAVITHRA S

(2617258012)

LIST OF ABBREVIATIONS

Ar	Aromatic
CADD	Computer Aided Drug Designing
DMBA	9, 12 - Dimethyl Benz[a]anthracene
DMSO	Dimethylsulphoxide
DCM	Dichloromethane
EGFR	Epidermal Growth Factor Receptor
ER	Estrogen Receptor
Fig	Figure
FTIR	Fourier transform infrared spectrometer
HDAC	Histone Deacetylase
HDACi	Histone Deacetylase inhibitor
HER2	Human Epidermal Receptor 2
¹ HNMR	Proton Nuclear Magnetic Resonance
IC ₅₀	Inhibitory Concentration
IGF	Insulin like Growth Factor
KD	KiloDalton
KBr	Potassium Bromide
mg	Milligram
min	minute
ml	Milliliter
mm	Millimeter

ABBREVIATIONS

MAPK	Mitogen activated Protein Kinase
MCF-7	Michigan Cancer Foundation-7
MDCK	Madin-Darby Canine Kidney Cells
MRI	Magnetic Resonance Imaging
MTT	(3-(4,5-dimethylthiazol-2-yl)-2,5-diphenyl tetrazolium bromide)
PARP	Poly ADP Ribose Polymerase
PDB	Protein Data Bank
PR	Progesterone Receptor
PSA	Polar Surface Area
p53	Cellular tumor antigen
SAHA	Suburanilamide hydroxamic acid
TLC	Thin Layer Chromatography
TNBC	Triple Negative Breast Cancer
UV-vis	Ultraviolet and visible spectroscopy
VEGF	Vascular Endothelial Growth Factor
VEGFR	Vascular Endothelial Growth Factor Receptor
ZBG	Zinc Binding Group
µg/ml	Microgram per liter
°C	Degree Celcius

TABLE OF CONTENTS

S.No	CONTENT	PAGE NUMBER
1	INTRODUCTION	1-14
2	LITERATURE REVIEW	15-20
3	AIM AND OBJECTIVE	21
3A	PLAN OF THE STUDY	22-24
4	MATERIALS AND METHODS	25-69
5	RESULTS AND DISCUSSION	70-75
6	CONCLUSION	76
7	BIBLIOGRAPHY	77-81

LIST OF TABLES

Table: 1	Component of Glide Score Docking (Extra-Precision Mode).....	28
Table: 2	Structure, Code and Docking results.....	31
Table: 3	Ligands and their interaction with binding sites.....	48
Table: 4	Qikprop Results of designed ligands.....	50
Table: 5	Physical properties of synthesized compounds.....	61
Table: 6	UV-vis spectral data of synthesized compounds.....	62
Table: 7	NMR spectral data of Compound EH03.....	64

LIST OF FIGURES

Fig: 1	HDAC inhibitors development.....	13
Fig: 2	FDA approved quinazolines.....	14
Fig: 3	Design of ligands.....	24
Fig: 4	STRUCTURE OF PROTEIN HDAC (PDB ID:1T69).....	29
Fig: 5	STRUCTURE OF PROTEIN EGFR (PDB ID:1XKK).....	30
Fig: 6	2D docked conformer of EH01 with EGFR (1XKK).....	42
Fig: 7	3D docked conformer of EH01 with EGFR (1XKK).....	42
Fig: 8	2D docked conformer of EH01 with HDAC (1T69).....	43
Fig: 9	3D docked conformer of EH01 with HDAC (1T69).....	43
Fig: 10	2D docked conformer of EH02 with EGFR (1XKK).....	44
Fig: 11	3D docked conformer of EH02 with EGFR (1XKK).....	44
Fig: 12	2D docked conformer of EH02 with HDAC (1T69).....	45
Fig: 13	3D docked conformer of EH02 with HDAC (1T69).....	45
Fig: 14	2D docked conformer of EH03 with EGFR (1XKK).....	46
Fig: 15	3D docked conformer of EH03 with EGFR (1XKK).....	46
Fig: 16	2D docked conformer of EH03 with HDAC (1T69).....	47
Fig: 17	3D docked conformer of EH03 with HDAC (1T69).....	47
Fig: 18	Synthesis Scheme of EH01.....	53
Fig: 19	Synthesis Scheme of EH02.....	55
Fig: 20	Synthesis Scheme of EH03.....	57
Fig: 21	NMR spectra of Compound EH 03.....	64

Fig: 22	Percentage inhibition of compound EH01	66
Fig: 23	Percentage inhibition of compound EH02.....	67
Fig: 24	Percentage inhibition of compound EH03.....	68
Fig: 25	% growth inhibition of Compound EH01.....	69

1. INTRODUCTION

Cancer is one of the most dangerous disorders worldwide. Cancer arises from the transformation of normal cells into tumour cells in a multistage process that generally progresses from a pre-cancerous lesion to a malignant tumour. These changes are the result of the interaction between a person's genetic factors and three categories of external agents, including:

- Physical carcinogens, such as ultraviolet and ionizing radiation
- Chemical carcinogens, such as asbestos, components of tobacco smoke, aflatoxin, and arsenic and
- Biological carcinogens, such as infections from certain viruses, bacteria, or parasites^[1]

It is the condition in which abnormal cells divide without control and can invade nearby tissues. Cancer cells can spread to other parts of the body through the blood and lymph systems.

Cancer is also a genetic disorder caused by changes in genes that control the way normal cells function, especially how they grow and divide.

The genetic changes that contribute to cancer tend to affect three main types of genes. They are

- Proto-oncogenes,
- Tumor suppressor genes, and
- DNA repair genes.^[2]

1.1 TYPES OF CANCER

There are various types of cancer which are named after their location of development (i.e) organ or tissue from which the cancer develops for example: Breast cancer, Colon cancer, Lung cancer, Hepatocellular Carcinoma etc., Even if the cancer spreads to other parts of the body and form secondary carcinomas they will be named after its primary cancer location.

Cancer can be broadly classified into many types based on the type of cell on which the cancer occurs. They are

1.1.1 CARCINOMA

This is the most common type of cancer. It develops mainly from the epithelial cells. Based on the specific epithelial cell carcinoma is of different types like,

- Adenocarcinoma – if formed in epithelial cells that produce fluid or mucus. eg) Breast, Colon and Prostate are adenocarcinomas.
- Basal cell carcinoma – if formed in the lower or basal layer of epidermis.
- Squamous cell carcinoma – if formed in squamous cells.
- Transitional cell carcinoma – if formed in transitional epithelium or urothelium. Eg) Bladder or kidney cancers are transitional cell carcinoma.

1.1.2 SARCOMA

These types of cancer forms in bones, joints and soft tissues Eg) Osteosarcoma, liposarcoma, Kaposi sarcoma, etc.,

1.1.3 LEUKEMIA

It is the type of cancer which is formed in blood forming tissues. These are not solid tumors.

1.1.4 LYMPHOMA

It is formed in lymphocytes (T or B cells). Two main types of lymphoma are Hodgkin lymphoma and Non-Hodgkin lymphoma.

1.1.5 MULTIPLE MYELOMA

It forms in plasma cells. The abnormal plasma cells are called myeloma cells.

1.1.6 MELANOMA

It is the cancer formed in melanocyte cells. Mostly melanomas forms in skin but can also form in pigmented tissues like eye.

1.1.7 BRAIN AND SPINAL CORD TUMORS

The cancers of brain and spinal cord are classified based on the specific cells.
Eg) Astrocytic tumor.

1.1.8 GERM CELL TUMOR

If formed in the germ cells (the cells that forms sperm or eggs) ^[2]

1.2 CANCER PREVALENCE AND INCIDENCE

Cancer is the second most common disease in India responsible for maximum mortality with about 0.3 million deaths per year. ^[5]

According to IARC (International Agency for Research on Cancer), WHO report on September 2018, “Cancer burden rises to 18.1 million new cases and 9.6 million cancer deaths in 2018”. The most common cancers are:

Lung (2.09 million cases)

Breast (2.09 million cases)

Colorectal (1.80 million cases)

Prostate (1.28 million cases)

Skin cancer (non-melanoma) (1.04 million cases)

Stomach (1.03 million cases) ^[1]

As per Indian population census data, the rate of mortality due to cancer in India was high and alarming with about 806,000 existing cases by the end of the last century.

Breast cancer is the first common cancer in females with prevalence rate 25.8 per 100,000 women and mortality rate 12.7 per 100,000 women in India. The age adjusted incidence rate was 41 per 100,000 for Delhi, 37.9 per 100,000 for Chennai, 34.4 per 100,000 for Bangalore. It was projected that as the prevalence of breast cancer may go upto 1797900 cases in India. ^[6]

Around one third of deaths from cancer are due to the 5 leading behavioral and dietary risks: high body mass index, low fruit and vegetable intake, lack of physical activity, tobacco use, and alcohol use. ^[1]

1.3 BREAST CANCER

Lung, prostate, colorectal, stomach and liver cancer are the most common types of cancer in men, while breast, colorectal, lung, cervix and thyroid cancer are the most common among women. ^[3]

Breast cancer is the second most common cancer in women. It is a cancer that forms in the cells of breasts.

1.3.1 SIGNS AND SYMPTOMS

Symptoms of breast cancer include

- Lump in the breast,
- Bloody discharge from the nipple,
- Changes in the shape or texture of the nipple or breast,
- Breast discomfort,
- Inverted nipple etc.,

1.3.2 RISK FACTORS

- Age (Risk increases with increase in age above 60 years)
- Personal history of invasive breast cancer, Ductal Carcinoma insitu (DCIS) or Lobular Carcinoma insitu (LCIS), Benign Breast disease
- Heredity
- Dense breast
- Exposure to oestrogen
- Hormone therapy for menopause symptoms
- Radiation therapy
- Obesity etc.,

1.3.3 STAGES OF BREAST CANCER

The most widely used method for staging of breast cancer is TNM system.

- T- Stands for Tumor size,
- N - Stands for Number and Location of lymph nodes with cancer.
[Lymph Node Status]
- M - Stands for Metastases

The other measures which were added more recently in 2018 are:-

- Tumor grade
- Estrogen - receptor status
- Progesterone receptor levels in the tumor tissue
- HER2/Neu Status
- Menopausal Status
- General health of the patient.^[4]

1.3.4 DIAGNOSIS

The breast cancer can be diagnosed by various techniques. The choice of diagnostic test is made based on the

- Type of cancer suspected
- Signs and symptoms
- Age and general health
- Results of earlier medical tests

The diagnosis tests mainly fall into four categories. They are imaging, biopsy, blood tests and genomic tests.

1.3.4.1 IMAGING TESTS

MAMMOGRAPHY – Mammogram is an X-ray of the breast. It may be screening or diagnostic mammogram based on the purpose for which it is done. Compared to screening mammogram, diagnostic mammograms provide more detailed results as they view the breast from multiple vantage points.

The reliability of mammogram is based on the size of the tumour, density of breast tissue as well as based on the skill of radiologists administering and reading the mammogram.

ULTRASOUND – A breast ultrasound is a scan that uses penetrating sound waves which deflects and causes echoes.

It provides evidence about whether the lump is a solid mass (may be cancerous tumor), a cyst filled with fluid (non cancerous), or a combination of the two. It is used to obtain information about exact size, location of lump and surrounding tissues.

MRI - An MRI uses magnetic fields, to produce detailed images of the body. A special dye called a contrast medium is given before the scan to help create a clear picture of the possible cancer. This dye can be injected into a patient's vein or given as a pill or liquid to swallow.

A breast MRI may be used to check how much the disease has grown throughout the breast and to differentiate a solid tumor.

1.3.4.2 BIOPSY

A breast biopsy is a test that involves removal of tissues from suspected area of the breast and examining under microscope. The types of breast biopsy are: Fine-needle aspiration biopsy, Core-needle biopsy and Surgical biopsy (wide local excision or lumpectomy). The type of biopsy is selected based on the appearance, size and location of the suspicious area on the breast.

It is the most accurate test for the diagnosis of breast cancer.

1.3.4.3 LAB TESTS

These additional lab tests are done to assist with prognosis. The lab test involves testing of hormone receptors and HER2/neu receptors on the cancer tissue using Immunohisto chemical analysis.

The results provide idea about selection of effective treatment option, viz. If the result is hormone receptor positive then hormonal therapy can be selected. If it is HER2/neu receptor positive suitable treatment option can be selected.

1.3.4.4 GENOMIC TESTS

It looks for specific genes or proteins that are found in cancer cells. The common genomic tests are:

- Oncotype Dx – for patients with ER-positive and PR-positive, HER2-negative breast cancer that has not spread to the lymph nodes. This test looks at 16 cancer-related genes and 5 reference genes to calculate a “recurrence score” that estimates the risk of the cancer coming back within 10 years after diagnosis. The recurrence score is used to guide recommendations on the use of chemotherapy.
- MammaPrint – for patients with ER-positive and PR-positive, HER2-negative breast cancer that has not spread to the lymph nodes or has only spread to 1 to 3 lymph nodes. This test uses information from 70 genes. The recurrence score is used to guide recommendations on the use of chemotherapy.
- Breast Cancer Index - for patients with ER-positive and PR-positive, HER2-negative breast cancer that has not spread to the lymph nodes. The results guide the details about duration of hormonal therapy needed for the particular patient.

It helps in personalization of the treatment. It also estimates the risk of cancer recurrence. [4, 7]

1.4 TREATMENT OF BREAST CANCER

- Surgery
- Radiation
- Hormone therapy
- Chemotherapy
- Targeted therapy

1.4.1 SURGERY

It involves the removal of tumor or nearby margins. If the patient is in stage 2 or 3, then chemotherapy is given as pre-operative or neo-adjuvant therapy.

The surgery may be lumpectomy (removal of only cancer cells and margins) or mastectomy (removal of entire breast) based on the condition of disease progression.

1.4.2 RADIATION THERAPY

Radiation therapy uses high-energy rays to kill cancer cells. It is used three to four weeks after surgery to destroy any remaining mutated cells that remain in the breast or armpit area. Breast cancer radiation therapy may be

- External Beam Breast Cancer Radiation (Traditional cancer-killing rays delivered by a large machine)
- Internal Breast Cancer Radiation (Newer treatments that inject radioactive cancer-killing treatments only in the affected area)
- Brachytherapy (Internal Radiation) Delivered Via Implantable Device

1.4.3 HORMONE THERAPY

It is recommended for the patients with hormone receptor positive. It involves blocking or inhibition of the hormonal receptors like estrogen receptor and progesterone receptor.

The drugs include

- Tamoxifen
- Toremifene
- Fulvestrant

Aromatase inhibitors:

- Anastrozole
- Exemestane
- Letrozole

1.4.3 CHEMOTHERAPY

This method uses a combination of drugs to either destroy cancer cells or slow down the growth of cancer cells.

- Anthracyclines, such as doxorubicin (Adriamycin) and epirubicin (Ellence)
- Taxanes, such as paclitaxel (Taxol) and docetaxel (Taxotere)
- 5-fluorouracil (5-FU)
- Cyclophosphamide (Cytosan)
- Carboplatin (Paraplatin), etc.,^[4]

1.5 TARGETED THERAPY

The different treatment strategies have various advantages and disadvantages on its own. The targeted therapy is the most advanced strategy which target specific genes or proteins which are over or under expressed in cancer condition. Several targets have been identified for cancer treatment and they are under investigation for their role in cancer development. Some common targets are: EGFR & HER2, VEGF, RAS/MEK/ERK pathway, PI3/AKT/mTOR pathway, IGF, PARP etc.,^[8] HDAC is also an important enzyme which is over expressed in many types of cancer.

1.5.1 OVERCOMING CHALLENGES

The problem with targeted therapeutics when targeting single target are:

- Development of resistance
- Multi-component drugs or drug cocktails
- Poor patient compliance,
- Unpredictable pharmacokinetic/ pharmacodynamic profiles
- Drug-drug interactions.

Dual targeting of different targets at the same time can control cancer prognoses and overcome the drawbacks of single target drug. Hence, dual targeting strategy is of great advantage than single target drugs.

The targets selected for dual targeting are:

- EGFR and
- HDAC

1.6 RESEARCH ENVISAGED

1.6.1 EGFR

Epidermal Growth Factor Receptor belongs to the ErbB tyrosine kinase receptor family. These are tyrosine kinase receptors which on binding of ligand undergo homodimerization or heterodimerization and activate a series of cellular signalling cascade. The signalling cascade includes activation of Ras/MEK/Erk pathway and PI3K/Akt/mTOR pathways which influences cell proliferation and apoptosis.

Several mechanisms lead to the receptor's aberrant activation observed in cancer, including receptor over-expression, mutation of ligand-receptor dimerization and ligand independent activation.

EGFR is a 170KD glycoprotein, which is commonly expressed in normal and malignant tissues and is involved in cellular communication. The receptors of the EGF family are composed of an extracellular domain, a hydrophobic transmembrane region and a tyrosine kinase-containing cytoplasmic region. The classical EGFR receptor is also known as HER-1 (human epidermal growth factor receptor 1) or ERBB-1 (v-erb-b2 erythroblastic leukemia viral oncogene homolog 1). The other members of EGF family are ERBB2 (also termed HER2 or HER2/neu), ERBB3 (also termed HER3), and ERBB4 (also termed HER4), they all share the same molecular structure. EGFR, when situated in the transmembrane position, has an extracellular domain, which provides a ligand-binding site for EGF and transforming growth factor-alpha (TGF- α). The intracellular domain of EGFR is activated upon ligand binding triggering the EGF-mediated tyrosine kinase signal transduction pathway.

EGF and TGF- α are believed to be the most important ligands for EGFR. Ligand binding with EGFR results in receptor homo- or heterodimerization at the cell surface followed by internalization of the dimerized receptor. After dimerization,

phosphorylation of the intracytoplasmic EGFR tyrosine kinase domain occurs. Phosphorylated tyrosine kinase residues serve as binding sites for the recruitment of signaling molecules, such as RAS (Rat Sarcoma Viral Oncogene). These signalling molecules have the ability to phosphorylate other “downstream” molecules. The activation of downstream pathways promotes cellular proliferation, angiogenesis, development of metastases and reduces apoptosis.

Ligand binding to epidermal growth factor receptors (EGFRs) and their subsequent dimerization induces receptor auto-phosphorylation. Several tyrosine-based motifs recruit a number of signal transducers to the phosphorylated form of EGFR (such as the adaptor proteins growth-factor-receptor bound-2 (GRB2) and Src-homology-2-containing (Shc), which are responsible for the recruitment of Ras and activation of the mitogen activated protein kinase (MAPK) cascades. Another direct substrate of ERBB1 is the signal transducer and activator of transcription-5 (STAT5).

The C terminus of ERBB1 contains a recognition site for the ubiquitin ligase Cbl, whereas no site is found that can directly recruit the lipid kinase phosphatidylinositol 3-kinase (PI3K). Consistent with the specificity of its docking sites, EGFR cannot directly activate the PI3K–AKT/protein kinase B (PKB) pathway, but it couples to the RAS–MAPK pathway, as well as to the RAS–PI3K–AKT/PKB pathway. EGFR signaling is negatively regulated through ubiquitylation by Cbl. The ERK cascade is regulated by intrinsic positive and negative feedback (for example, ERK negatively feeds back to RAF) and extrinsic crosstalk regulation from other kinase cascades.

In breast cancer, EGFR is overexpressed or mutant forms are able to manipulate downstream signaling. One way to manipulate the EGFR network entails setting the level of activity just below the threshold required for the mobilization of control machineries. For example, mutant forms of EGFR frequently detected in lung cancer are characterized by a basal, ligand-independent function, which is sufficient to weakly activate downstream signals but insufficient to recruit CBL to trigger receptor degradation [13].

Almost 40% of Triple Negative Breast Cancer has EGFR over expression. It reveals that EGFR can be targeted even in the severe cases like TNBC. Hence, targeting a EGFR can control the cancer proliferation.^[9]

1.6.2 HDAC

Histone deacetylases (HDAC) are involved in cellular processes and the regulation of gene expression through the control of protein acetylation. The over expression of HDAC proteins resulted in unregulated transcription and aberrant protein activity and function which is linked to several diseases including cancer.

The HDAC enzymes are a group of enzymes divided into 4 classes depending on sequence homology. The members of these classes are:

- Class I - HDAC 1, 2, 3 and 8,
- Class IIA - HDAC 4, 5, 7 and 9,
- Class IIB - HDAC 6 and 10,
- Class III - Sirutins in mammals (SIRT 1 - 7),
- Class IV - HDAC 11.

These all proteins are metal dependent.

HDACs, that may be called protein deacetylases (PDAC) as some of their targets are non-histone proteins. These a family of eleven zinc-dependent enzymes that have gained major interest as therapeutic targets, mainly in cancer research. Their abnormal expression in many cancer cells modifies the expression of tumour suppressor genes (TSG) and genes involved in normal cellular functions.^[10] In addition, HDAC proteins influence protein-protein interaction, protein - DNA interaction, protein localization and protein stability through deacetylation of non-histone substrates. ^[11]

Different members of this class of enzyme are over-expressed in different types of cancer. For example: HDAC 1 in lung, breast and colon cancer. HDAC 2 in colorectal cancer. HDAC 6 in oral squamous cell carcinoma and ovarian cancer. Over

expression of both HDAC 6 and 8 was linked to breast cancer metastasis and invasion. [11]

Various HDAC inhibitors have been developed as anticancer agents which promoted apoptosis and reduced proliferation and migration through their effects on both histone and non - histone substrates. SAHA (Suberoylamide hydroxamic acid or Vorinostat) is a FDA approved drug as non-selective HDAC inhibitor. Many drugs have been designed by modifying the SAHA nucleus to improve selectivity as to reduce the side effects due to its non-selectivity.

The basic HDAC enzyme inhibitor has three major parts. They are the capping group, linker region and a metal binding group. Difference in these regions or groups has effects in modifying the selectivity and potency of HDAC inhibitors.

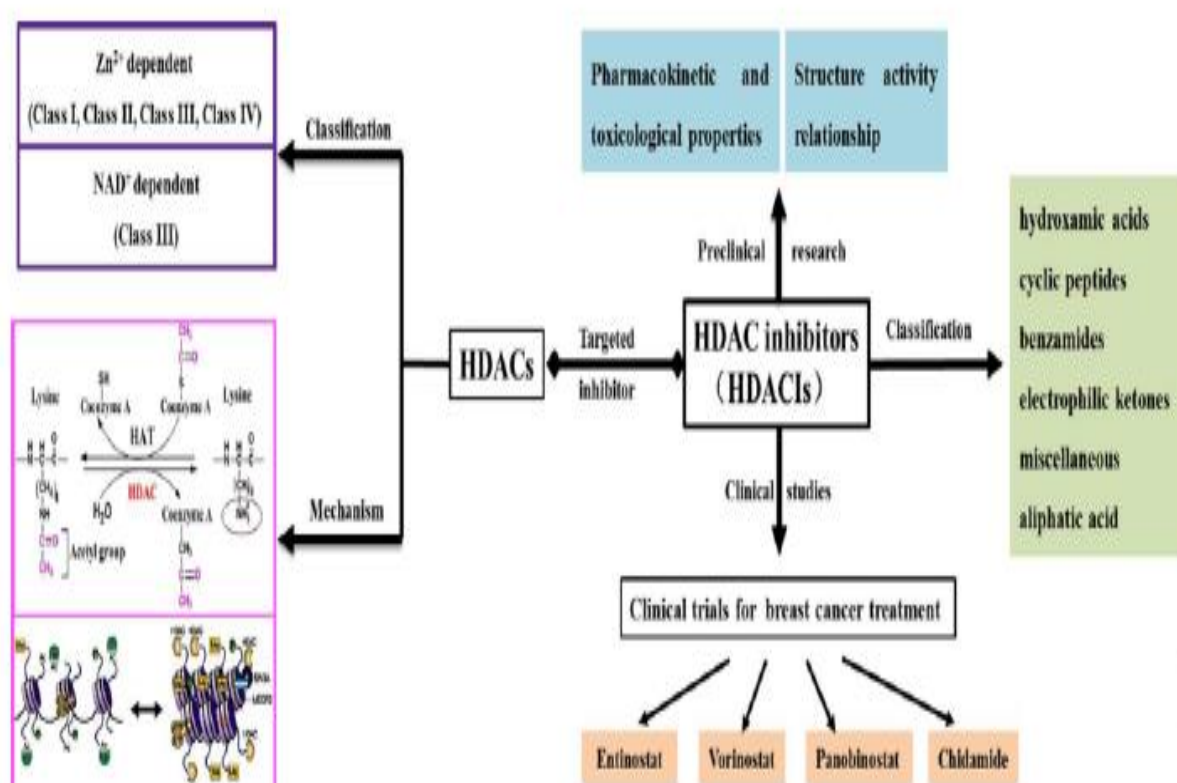


Fig 1 : HDAC inhibitors development

1.6.3 DESIGNED DUAL INHIBITOR

Quinazoline scaffold has been widely used as anti-cancer, anti-malarial, anti-bacterial, anti-inflammatory, anticonvulsant and anti-diabetic agents. Many quinazoline drugs have been approved by USFDA as potential anticancer agents.^[11]

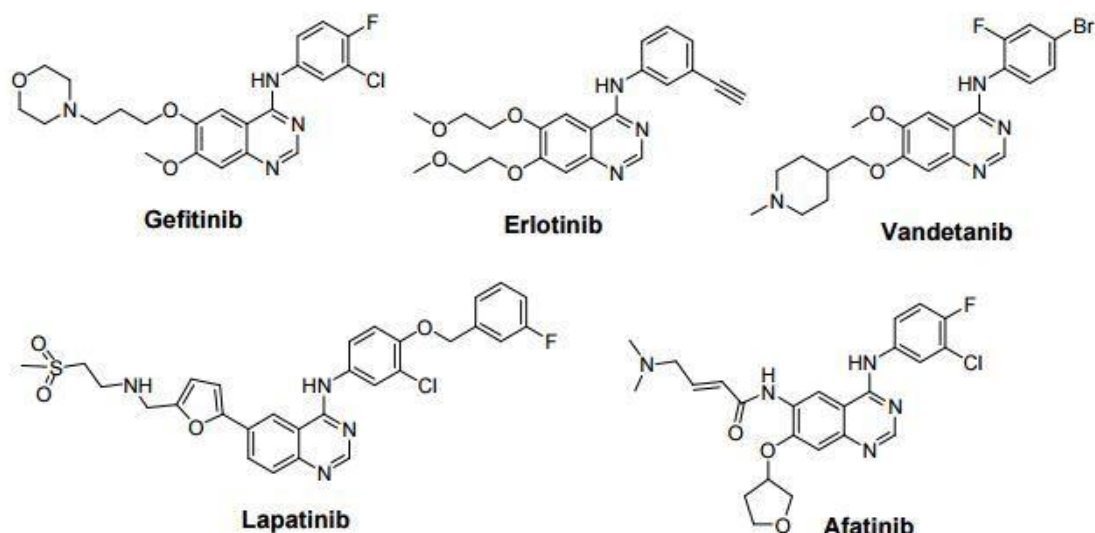


Fig 2: FDA approved quinazolines

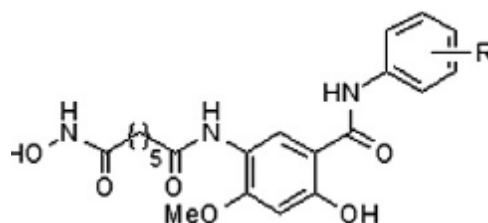
The use of quinazolines as the basic scaffold and combining it with the pharmacophore of HDAC can be of advantage in designing a dual inhibitor for EGFR and HDAC.

2. LITERATURE REVIEW

Ricardo H. Alvarez *et.al.*,(2010)^[14] reviewed the possible targets of breast cancer and the emerging targeted therapies. The role of various targets like EGFR & HER2, VEGF, RAS/MEK/ERK pathway, PI3/AKT/mTOR pathway, IGF, PARP etc., has been described. This review focused on these targets and the effective drugs available in the market for modulating these targets.

Xinyu Li *et.al.*, (2019)^[15] designed a series of 3-aryl-quinolin derivatives to target ER α and VEGFR-2 for anti-breast cancer activity. The 3-aryl-quinazoline derivative substituted with piperazinyl showed high ER α binding affinities as well as relative intensity VEGFR-2 inhibitory activities. And also exhibited excellent anti-proliferative activities against MCF-7 and HUVEC cell lines with low micro-molar IC₅₀ (1–8 μ M). They also found that they can also reduce the expression of PgR mRNA, arrest cell cycle in MCF-7 breast cancer cells, and restrain the cell migration.

Miao Zuo *et.al.*, (2012)^[16] synthesized N-aryl salicylamides with a hydroxamic acid moiety at 5-position and evaluated against EGFR and HDAC. All compounds displayed inhibitory activity. Their anti-proliferative activities were evaluated by MTT assay against human cancer cell lines A431, A549 and HL-60. The results showed that ether linker compound was more potent than amide linker compound against A431 and A549. Compounds with halogen substituent's and with methoxy substituent exhibited higher potency against HL-60 than standards (Gefitinib & SAHA). It was found that by combining two distinct pharmacophores into one molecule, dual inhibition can be achieved.



R = 3-Cl, 4-F

Bruna Zucchetti et.al., (2018) ^[17] reviewed the role of HDAC inhibitors in the Metastatic breast cancer. HDAC inhibitors represent also a potential combination therapy with other agents (as immunecheckpoint inhibitors) in patients with metastatic TNBC. Although much progress had been made in the HDACi field, it is still not completely clear how effective they are for solid tumors and our ability to identify the responding tumors is limited by our poor understanding of the mechanism that underlies its effectiveness. They summarized the latest studies with HDACi in breast cancer

Gopi Reddy et.al., (2017) ^[18] reviewed the role of Quinazolines as anticancer agent. The review showed that quinazoline moiety has great biological and medicinal significance. The possible improvements in the activity can be achieved by slight modifications in the substituents on the basic quinazoline nucleus. Various recent new drug developments in quinazoline derivatives show better effect and less toxicity. This study gives valuable information for further development of more potent anticancer agents.

Xiong Cai et.al., (2010)^[19] designed novel quinazoline derivatives by incorporating the incorporating the pharmacophore for HDAC inhibition in the EGFR and HER2 inhibitors pharmacophore and identified that the compound 7-(4-(3-Ethynylphenylamino)-7-methoxyquinazolin-6-yloxy)-N-hydroxyheptanamide as a drug candidate. This compound showed potent *in-vitro* activity against all EGFR, HER2 and HDAC in nM range. In *in vivo* it promotes tumor regression or inhibition in various cancer xenograft models including non- small cell lung cancer (NSCLC), liver, breast, head and neck, colon and pancreatic cancers. Now this compound CUDC 101 had entered the clinical trial also.

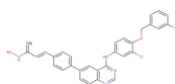
Chao Ding et.al., (2017)^[20] designed novel 6-(1,2,3-triazol-4-yl)-4-aminoquinazolin derivatives as multi-target inhibitors against EGFR, HER2 and HDAC. All the compounds showed good inhibitory activity on *in-vitro* enzyme inhibition assay. The

LITERATURE REVIEW

cytotoxicity studies against various cell lines like A549, A431, BT474, SK-Br-3, NCI-H-1975 showed inhibition in micromolar ranges. The flow cytometry study also revealed that the compounds can induce apoptosis upto 63.86%. Hence, the dual inhibition can be achieved possibly by combining the two distinct pharmacophors of EGFR and HDAC inhibitors.

Er-dong Li et.al., (2019)^[21] designed a series of novel 2,4-disubstituted quinazolines and evaluated their anti-tumor activity against five human cancer cells (MDA-MB-231, MCF-7, PC-3, HGC-27 and MGC-803) using MTT assay. Among them, compound 9n (tri-fluoro methyl derivative) showed the most potent cytotoxicity against breast cancer cells. And also induced cell cycle arrest at G1 phase and cell apoptosis, as well as increased accumulation of intracellular ROS. Furthermore, it exerted anti-tumor effects in vitro via decreasing the expression of anti-apoptotic protein Bcl-2 and increasing the pro-apoptotic protein Bax and p53. Mechanistically it markedly decreased p-EGFR and p-PI3K expression.

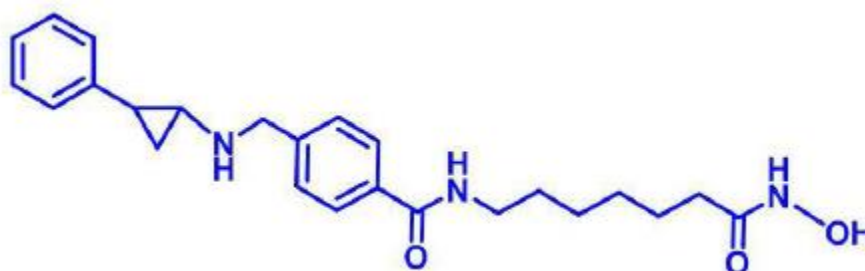
Sivosh Mahaboobi et.al., (2010)^[22] designed and synthesised a series of lapatinib hybrids. They combined the inhibitory head group of HDAC enzyme viz, hydroxamic acid and benzamide motifs with the [3-chloro-4-(3-fluorobenzyloxy)-phenyl]-quinazolin-4-yl-amine core structure to target EGFR, HER2 proteins. The enzyme inhibition assay, cell proliferation assay and cytotoxicity studies showed good potency to both targets. In which the compound 6c showed better activity against all the targets.



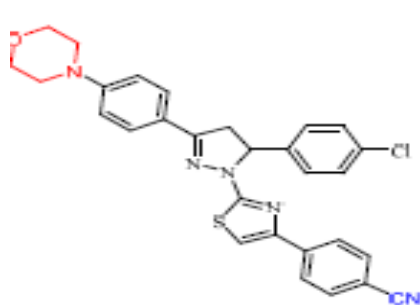
Compound 6c

Weiwei Yu et.al.,^[23] developed a combined therapy of histone deacetylase inhibition by a novel HDAC inhibitor, YF454A, with erlotinib to overcome EGFR-TKI resistance. The sensitization of erlotinib by YF454A was examined. Western blotting and Affymetrix GeneChip expression analysis were further performed to determine underlying mechanisms for the combinatorial effects. YF454A and erlotinib showed a strong synergy in the suppression of cell growth by blocking the cell cycle and triggering cell apoptosis in EGFR-TKI-resistant NSCLC cells. The combined treatment led to a significant decrease in tumor growth and tumor weight compared with single agents alone. Mechanistically, this combination therapy dramatically down-regulated the expression of several crucial EGFR-TKI-resistance-related receptor tyrosine kinases, such as Her2, c-Met, IGF1R and AXL, at both the transcriptional and protein levels, and consequently blocked the activation of downstream molecules AKT and ERK. Transcriptomic profiling analysis further revealed that YF-454A and erlotinib synergistically suppressed the cell cycle pathway and decreased the transcription of cell-cycle related genes, such as MSH6 and MCM7.

Ying-Chao Duan et.al., (2017)^[24] designed a dual inhibitor for Lysine specific demethylase 1 (LSD1) and Histone deacetylases (HDACs). The result evidenced a synergistic Effect of combined LSD1 and HDAC inhibitors on cancers. Therefore, development of inhibitors targeting both LSD1 and HDACs might be a promising strategy for epigenetic therapy of cancers. They reported a series of tranlycypromine derivatives as LSD1/HDACs dual inhibitors. The *N*-(7-(hydroxyamino)-7-oxoheptyl)-4-((phenylcyclopropyl)amino)methyl) Benzamide showed stronger antiproliferative effect against human cancer cell lines. It is well docked into the active binding sites of LSD1 and HDAC2

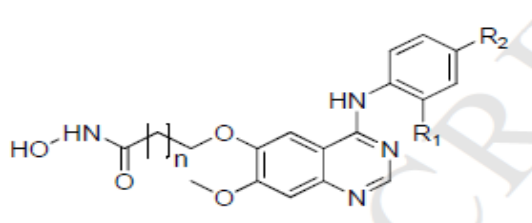


Belgin Sever *et al.*,^[25] designed a series of thiazolyl-pyrazolines as novel inhibitor for both HDAC and EGFR. The compound 1-(4-(4-cyanophenyl)thiazol-2-yl)-3-(4-morpholino phenyl) -5-(4-chlorophenyl)-2-pyrazoline showed good activity against both the targets *in-vitro*. This compound also shown good affinity with the ATP binding sites of EGFR and HDAC.



Meiling Huang *et al.*,^[26] reviewed the targets of breast cancer therapy. They have found that epigenetic abnormalities have emerged as an important hallmark of cancer development and progression. The HDACs mechanism and classification and their association between breast cancer has been reviewed and they found that the HDAC inhibitors have become promising potential anticancer drugs for research due to their crucial to chromatin remodeling and epigenetics. In conclusion they found that, HDACIs have shown desirable effects on breast cancer, especially when they are used in combination with other anticancer agents.

Fan-Wei Peng *et al.*,^[27] designed a series of hybrids bearing *N*-phenylquinazolin-4-amine and hydroxamic acid moieties as dual inhibitor for VEGFR-2 and HDAC. They combined the pharmacophore for both the targets and designed a dual inhibitor for acting on multiple targets to produce synergistic effect. The compound 7-(4-(4-bromophenylamino)-7-methoxyquinazolin-6-ylloxy)-*N*-hydroxyheptanamide showed greater activity against both the targets.

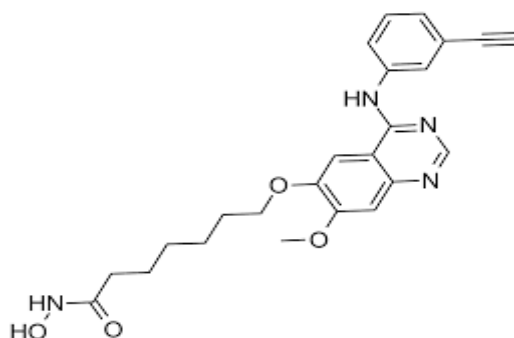


$$R_1 = H$$

$$R_2 = Br$$

$$n = 5$$

Shimizu *et al.*,^[28] reported the efficacy of multi-targeted drug CUDC-101 which is a synthetic small-molecule, first-in-class, multitargeted inhibitor of both receptor tyrosine kinases (RTK), EGFR and HER2, and class I/II HDACs. Along with these direct effects, CUDC-101 also indirectly attenuates the survival signaling pathways Akt, HER3, and MET. Through this inhibition of multiple signaling networks, CUDC-101 effectively suppresses the growth of a broad range of tumor types both in vitro and in vivo, including RTK-resistant cell lines.



3. AIM AND OBJECTIVES

AIM:

To design novel compound for modulating HDAC and EGFR over expression and evaluating its target specificity using CADD and screening *in-vivo* using animal model

OBJECTIVES:

- To design a series of novel compounds for targeting both the targets EGFR and HDAC simultaneously
- To evaluate the efficacy of designed compounds *in-silico* using CADD
- To evaluate the pharmacokinetic parameters of the designed compounds
- To synthesis the compounds with greater efficacy as well as pharmacokinetics
- To evaluate the efficacy of the synthesized compounds *in-vitro*
- To evaluate the effectiveness of the synthesized compounds *in-vivo*

3A. PLAN OF STUDY

Phase I: Literature Survey.

Phase II: Molecular modelling design a ligand for targeting EGFR and HDAC of cancer based on literature.

Phase III: Identification of best ligand/ligands based on DOCK score and LIPINSKI rule.

Phase IV: Screening of pharmacokinetic properties by maestro11.2 software.

Phase V: Synthesis of quinoxolone derivatives.

Phase V: The purity of the synthesised chemical entities to be monitored by thin layer chromatography and chemical structure to be assigned by various analytical techniques such as FTIR, H^1NMR .

Phase VI:

- Screening of the novel compounds against mammary cancer *in-vitro*

Phase VII:

- Screening of the novel compounds against mammary cancer *in-vivo* using DMBA induced mammary carcinoma model

Phase VIII: Result and discussion.

RESEARCH ENVISAGED

A single agent that simultaneously inhibits multiple targets may offer greater therapeutic benefits in cancer than single-acting agents through interference with multiple pathways and potential synergistic action.

EGFR is a receptor which is known to be over-expressed in a variety of cancer and its effect on breast cancer has also been proven and a variety of EGFR inhibitors having quinazoline scaffold is widely prescribed as anticancer agents.

HDAC (Histone Deacetylases) are also an enzyme involved in many important biological functions. They are also an important target for cancer research. The HDAC inhibitors are known to have three regions viz., Cap, Linker and Zinc binding group in their structure to be effective.

By combining these two pharmacophores we can design a series of compounds which can act on both the targets so that an effective drug molecule which can inhibit dual targets with high efficacy can be identified.

PLAN OF STUDY

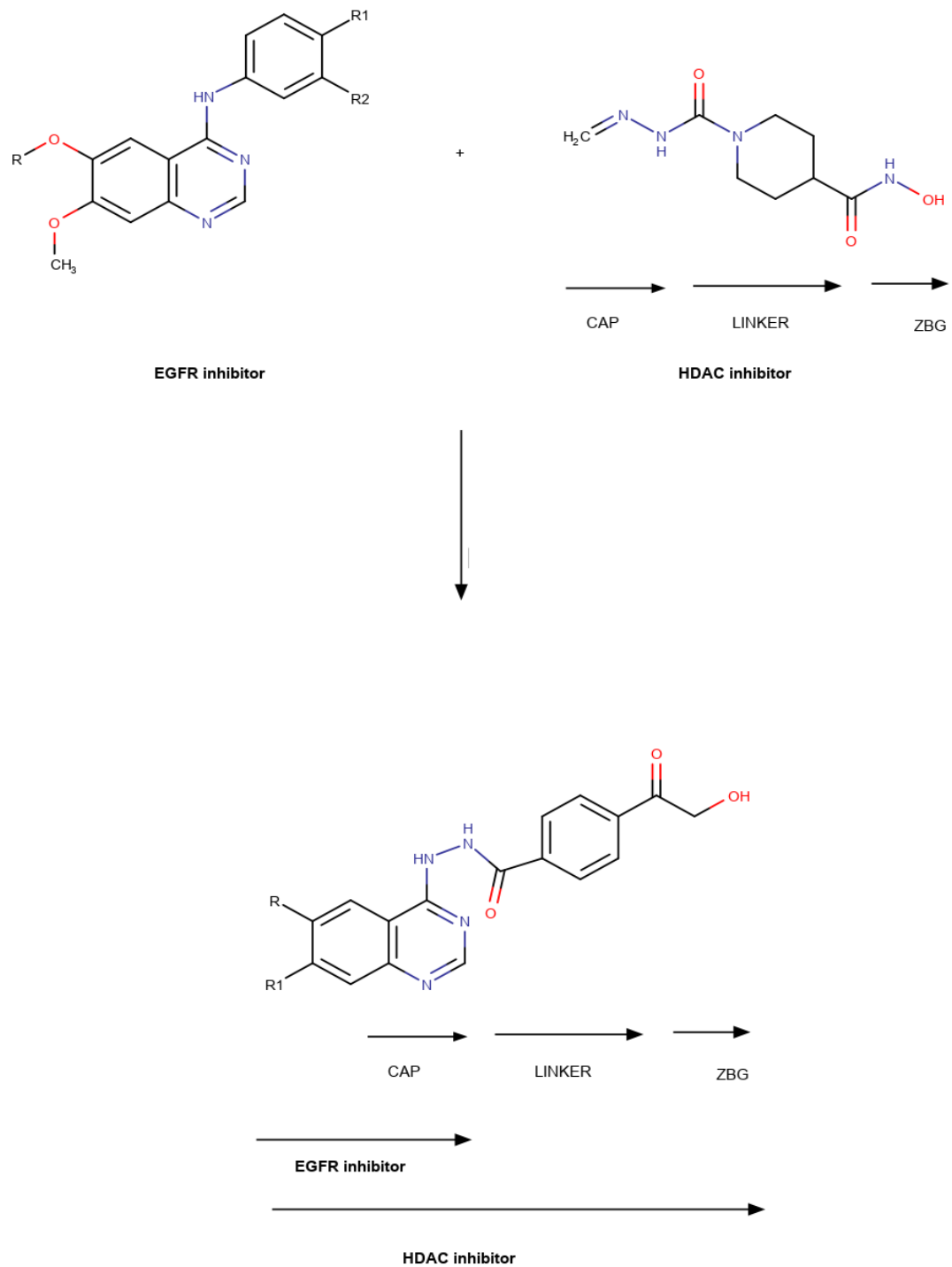


Fig: 3 Design of ligands

4. METHODOLOGY

4.1 DOCKING STUDIES

Glide docking uses the assumption of a rigid receptor, although scaling of vanderwaals radii of non polar atom, which decrease penalties for close contacts, can be used to model a light “give” in the receptor and/or ligand. Docking studies of designed compounds were carried out using GLIDE (Grid-based Ligand Docking with Energetics) module version 10.1, Schrodinger, LLC, New York, NY, 2015. The software package running on multi-processor running on multi-processor Linux PC, GLIDE has previously been validated and applied successfully to predict the binding orientation of many ligands.

4.1.1 DOCKING METHODOLOGY

The steps involved in docking are as follows:

Ligand Structure: The chemical structure of each ligand was drawn using build module.

Ligand Preparation: The 2D structures of the designed molecules were constructed using GLIDE 2D sketcher and then it was created in 3D structure format. LigPrep, a utility in Schrodinger software suite that combines tools for generating 3D structures. LigPrep produced a single, low-energy, 3D structure with correlated chiralities for each successfully processed input structures.

Preparation of Protein: The X-ray crystal structures of the proteins EGFR (PDB ID: 1T67) and HDAC (PDB ID: 1XKK) were obtained from the RCSB protein data bank (<http://www.rcsb.org/pdb>). After selection, the 3-Dimensional structures of the protein it was analysed for potential binding pockets and then prepared by docking software Schrodinger-Maestro 10.1. Usually the PDB structure consist of metal ions, cofactors, can contain waters and has no information on bond orders, formal atomic charges and misaligned terminal amide groups Ionization and tautomeric states. In order to acquire accurate energy evaluation the bond orders and ionization states to properly assigned, side chains to be reoriented and steric clashes to be relieved as Glide calculations are based on all-atom force field. The missing side-chain atoms were added manually and

the proteins were pre-processed separately by deleting the substrate cofactor as well as the crystallographic ally observed water molecules (water without H bonds), correcting the mistakes in PDB file, optimizing hydrogen bonds. After assigning formal charge with bond orders and protonation state finally energy minimization was done.

Receptor grid generation: Receptor grid generation requires a prepared structure: an all atom structure with appropriate bond order and formal charges. Glide searches for favourable interaction between one or more ligand molecules and a receptor molecule, usually a protein. The shape and properties of the receptor are represented on a grid by several different sets of field that provide progressively more accurate scoring of the ligand poses. The option in each tab of the Receptor Grid Generation panel allow defining the receptor structure by excluding any co-crystallized ligand that may be present, determine the position and size of the active site as it will be represented by receptor grid, and set up Glide constraints. A grid area was generated around the binding site of the receptor.

Ligand docking: This is carried out using GLIDE DOCK. Glide searches for favourable interaction between one or more ligand molecule and a receptor molecule, usually a protein. Each ligand acts as single molecule, while the receptor may include more than one molecule, eg., a protein and a cofactor. Glide a run in rigid or flexible docking mode; the latter automatically generated conformation for each input ligand. The combination of position and orientation of a ligand relative to the receptor, along with its conformation in flexible docking, is referred to as a ligand poses. The ligand poses that Glide generate pass through a series of hierarchical filter that evaluate the ligand to the defined active site and examine the complementarity of ligand-receptor interaction using a grid-based method patterned after the empirical chem. score function. Poses that passed the initial screen entered the final stage of the algorithm, which involve evaluation and minimization of a grid approximation to the OPLS-2005 non bonded ligand-receptor interaction energy. Final scoring is then carried out on the energy-minimised poses.

Glide Extra-Precision Mode (XP): The extra-precision (XP) mode of Glide combines a powerful sampling protocol with the use of a custom scoring function

designed to identify ligand poses that would be expected to have unfavourable energies, based on well-known principles of physical chemistry. The presumption is that only active compounds will have available poses that avoid these penalties and also receive favourable scores for appropriate hydrophobic contact between the protein and the ligand, hydrogen-bonding interactions, and so on. The chief purposes of the XP method are to weed out false positives and to provide a better correlation between good poses and good scores. Extra-precision mode is a refinement tool designed for use only on good ligand poses. Finally, the minimized poses are re-scored using Schrodinger's proprietary Glide Scores coring function. Glide Score is based on Chem Score, but includes a steric-clash term and adds buried polar terms devised by Schrodinger to penalize electrostatic mismatches:

$$\text{Glide Score} = 0.065 \cdot \text{vdW} + 0.130 \cdot \text{Coul} + \text{Lipo} + \text{Hbond} + \text{Metal} + \text{BuryP} + \text{RotB} + \text{Site}$$

Where, vdW – Vander Waal energy, Coul – Coulomb energy, Lipo – Lipophilic contact term, HBond – Hydrogen-bonding, term Metal – Metal-binding, Term BuryP – Penalty for buried polar groups, RotB – Penalty for freezing rotatable bonds, Site – Polar interactions at the active site and the coefficients of vdW and Coul are – a = 0.065, b = 0.1.

Table: 1 Components of Glide Score Docking (Extra-Precision Mode)

Component	Description
vdW	Vander Waals energy is calculated with reduced net ionic charges on groups with formal charges, such as metals, carboxylates and guanidiniums.
Coul	Coloumb energy is calculated with reduced net ionic charges on groups with formal charges, such as metals, carboxylates and guanidiniums.
Lipo	Lipophilic contact term. Rewards favourable hydrophobic interactions.
HBond	Hydrogen-Bonding term is separated into differently weighrd components that depend on whether the donor and acceptor are neutral, one is neutral and the other is charged, or both are charged.
Metal	Metal-binding term used only for the interactions with anionic acceptor atoms is included. If the net metal charge in the apo protein is positive, the preference for anionic ligands is included; if the net charge is zero, the preference is suppressed.
BuryP	Penalty for buried polar groups.
RotB	Penalty for freezing rotatable bonds.
Site	Polar interactions in the active site. Polar but non-hydrogen bonding atoms in the hydrophobic region are rewarded.

Docking Procedure:

The computational modeling studies relied upon the GLIDE (Grid-based ligand Docking from Energetics) program (Glide, version 5.0, Schrodinger, LLC New York, 2008) for the docking simulations. These simulations were performed using the X-ray crystal structure of the human HDAC 8 complexed with SAHA (PDB ID: 1T69) and EGFR (PDB ID: 1XKK). All the water molecules in the crystal structures were deleted, bond orders were assigned, hydrogen's were added and the protein was

then further refined for the docking studies by processing it using Schrodinger's Protein preparation wizard. This procedure minimizes the protein to 0.30Å RMSD using OPLS-2005 forcefield. Ligands were prepared using build panel in maestro.

PROTEIN INFORMATION:

Experimental Data:

Method: X-RAY DIFFRACTION
DIFFRACTION

Resolution: 2.91 Å

R-Value Free: 0.310

R-Value Work: 0.249

Experimental Data:

Method: X-RAY

Resolution: 2.4 Å

R-Value Free: 0.255

R-Value Work: 0.209

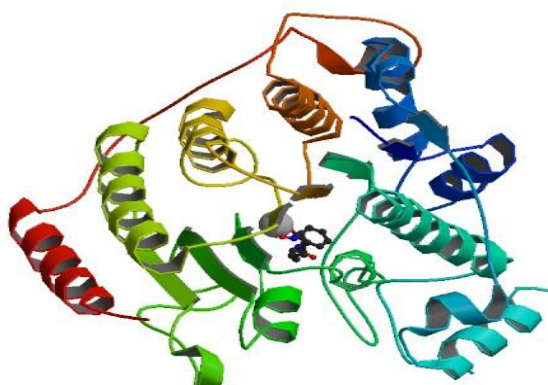


Fig: 4 STRUCTURE OF PROTEIN HDAC (PDB ID:1T69)

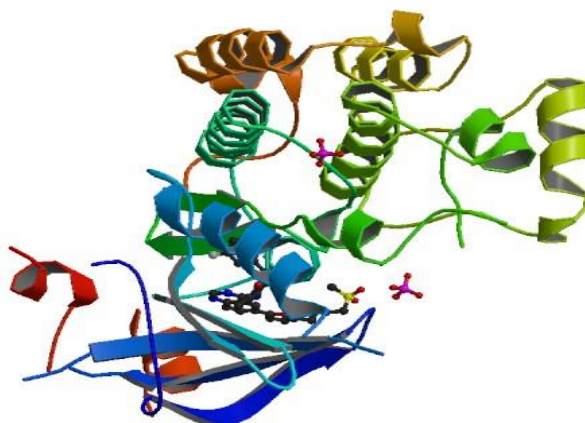
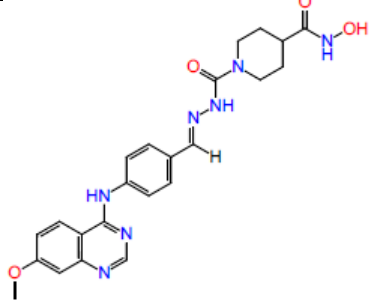
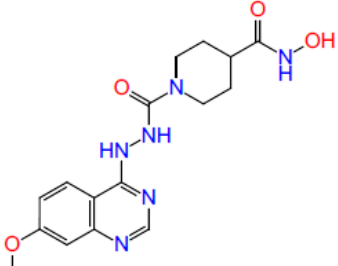
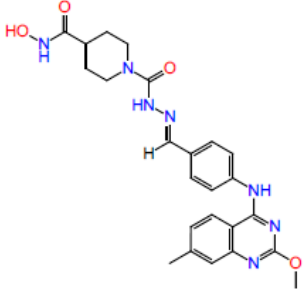
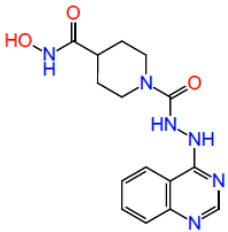
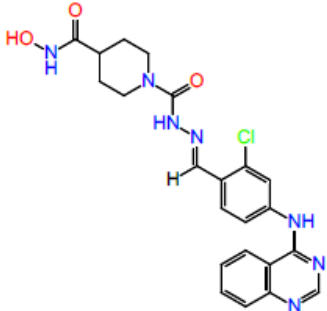


Fig: 5 STRUCTURE OF PROTEIN EGFR (PDB ID:1XKK)

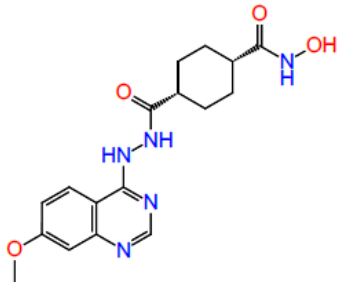
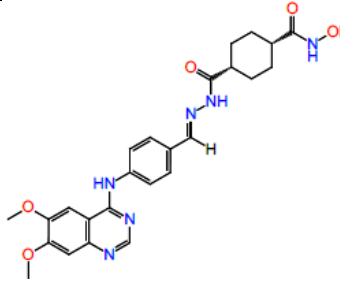
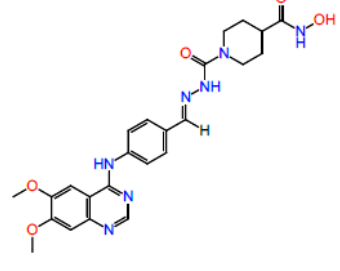
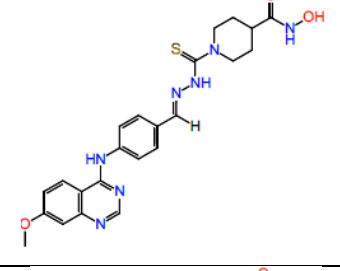
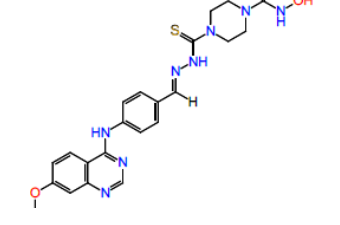
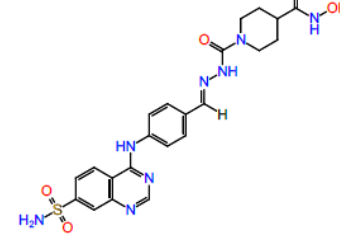
Further the ligands were prepared for docking using LigPrep tool and were energy minimized using MMFF Force Field. Glide Grid generation panel has been used to generate receptor grid for docking. Default SP (Standard Precision) docking protocol was used to dock the library ligands.

Molecular docking were performed for 60 compounds using the GLIDE program (Version 5.0, Schrodinger, LLC, New York, 2008) to understand the interaction of 3k with HDAC8. The Maestro user interface (version 8.5, Schrodinger, LLC, New York, 2008) was employed to set up and execute the docking protocol and also for analysis of the docking results. Human HDAC8 (PDB ID: 1T69) was selected for docking studies and was prepared for docking through protein preparation wizard, energy minimization has been carried out using OPLS 2005 forcefield. Structures of 60 compounds were sketched using built on Maestro and prepared for docking through Ligprep module (energy minimized using MMFF force field). GLIDE grid generation wizard has been used to define the docking space. Docking was performed using XP (Extra-Precision mode) docking protocol. The molecular docking results were presented in Table 2.

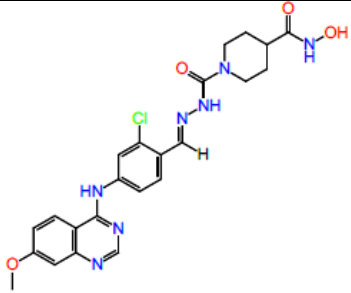
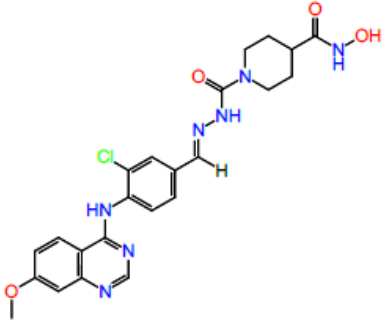
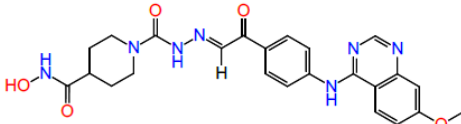
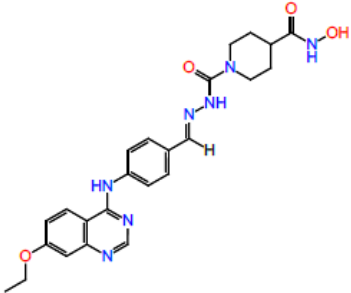
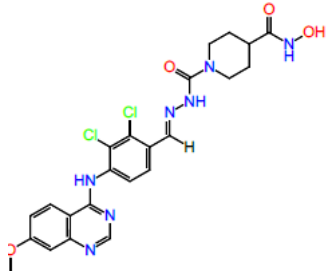
Table: 2 Structure, Code and Docking results

CODE	STRUCTURE	DOCKING RESULTS	
		1XKK	1T69
PV1		-8.313	-7.645
PV2		-9.287	-8.086
PV3		-5.56	-7.243
PV4		-9.779	-8.044
PV5		-7.578	-8.375

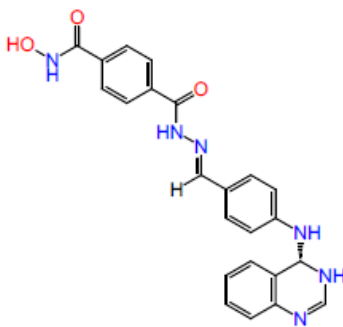
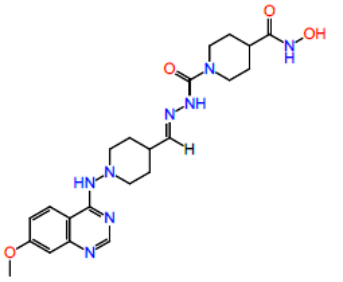
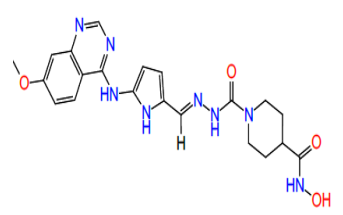
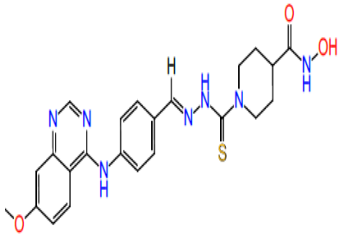
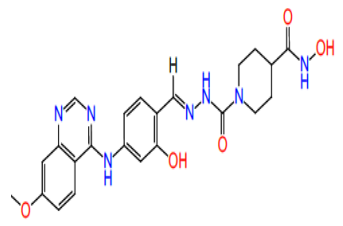
METHODOLOGY

PV6		-10.889	-8.492
PV7		-8.589	-4.155
PV8		-6.408	-2.893
PV9		-7.509	-3.463
PV10		-6.533	-2.039
PV11		-5.239	-7.508

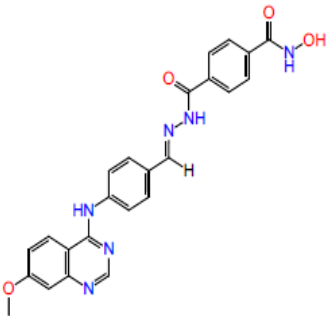
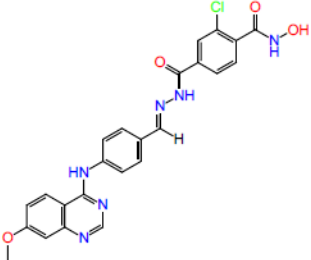
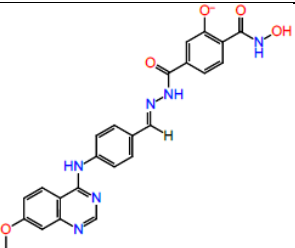
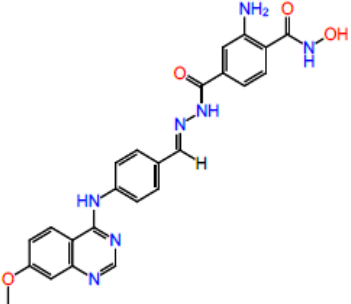
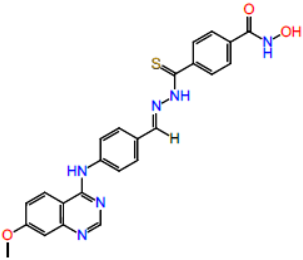
METHODOLOGY

PV12		-9.056	-3.393
PV13		-8.352	-3.72
PV14		-8.57	-6.288
PV15		-7.74	-5.706
PV16		-8.909	-4.305

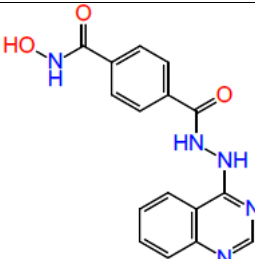
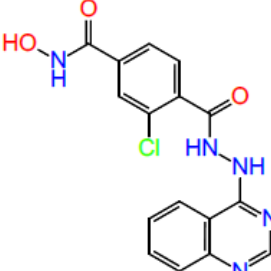
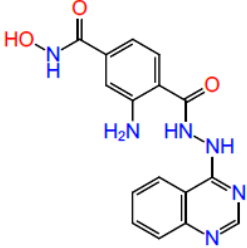
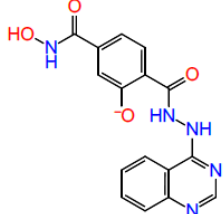
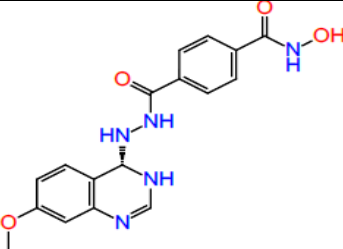
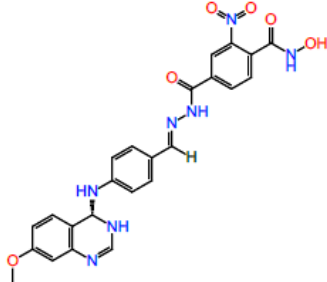
METHODOLOGY

PV17		-7.712	-6.402
PV18		-5.819	-7.995
PV19		-7.683	-6.733
PV20		-7.216	-2.935
PV21		-5.172	-2.747

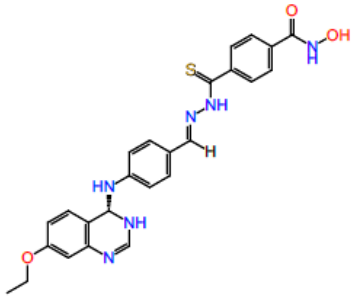
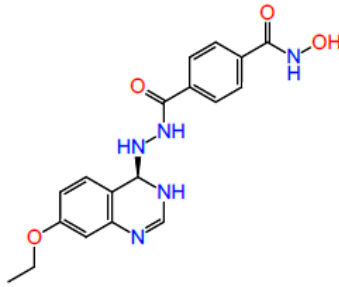
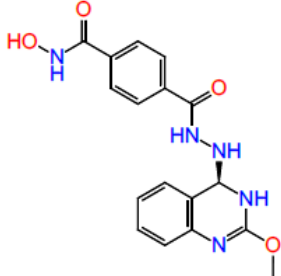
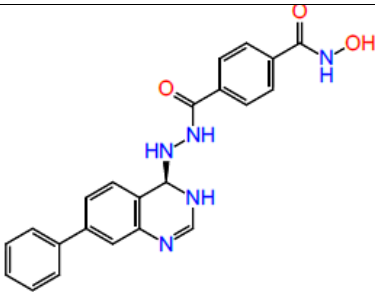
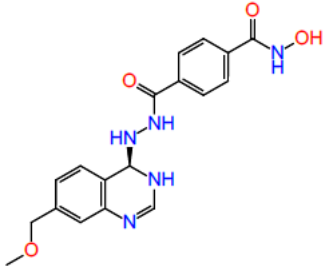
METHODOLOGY

PV22		-6.012	-7.956
PV23		-6.350	-2.681
PV24		-5.912	-5.915
PV25		-6.586	-3.464
PV26		-5.410	-5.873

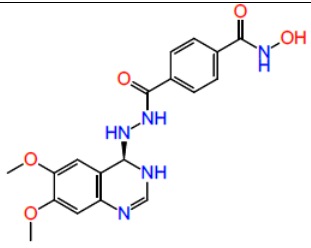
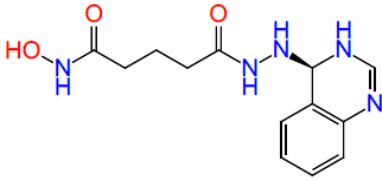
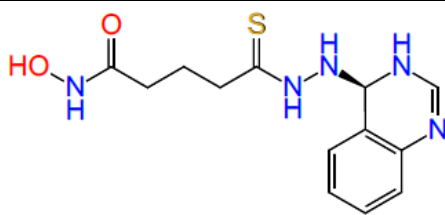
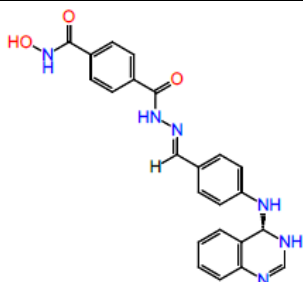
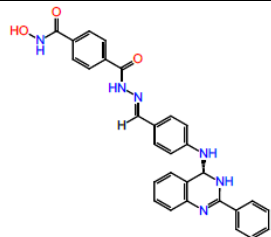
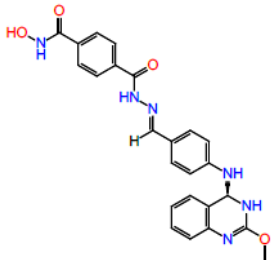
METHODOLOGY

PV27		-7.010	-8.854
PV28		-7.673	-8.993
PV29		-8.035	-8.747
PV30		-8.180	-9.115
PV31		-7.505	-8.848
PV32		-5.559	-9.319

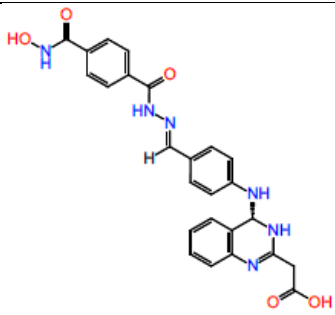
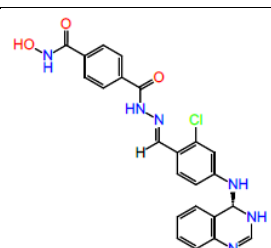
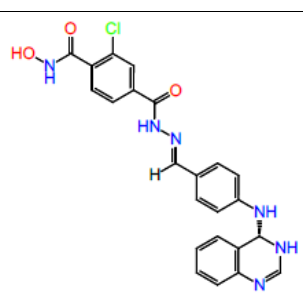
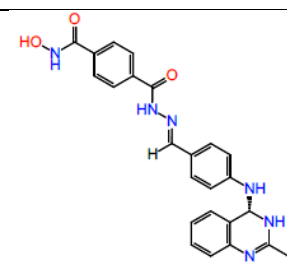
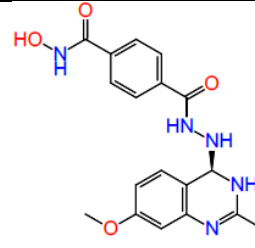
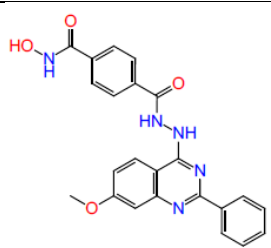
METHODOLOGY

PV33		-5.440	-5.440
PV34		-6.818	-8.901
PV35		-7.491	-8.806
PV36		-7.832	-8.685
PV37		-7.248	-9.962

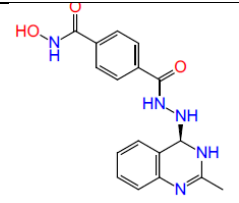
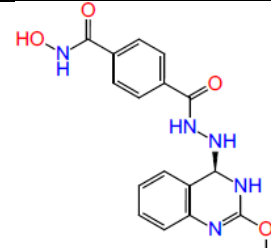
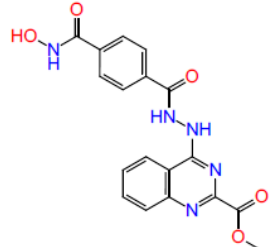
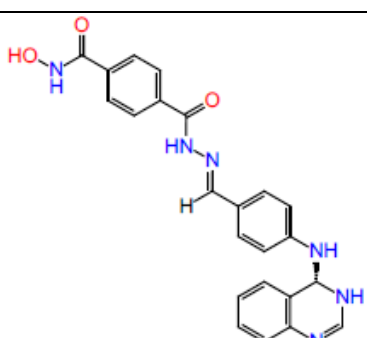
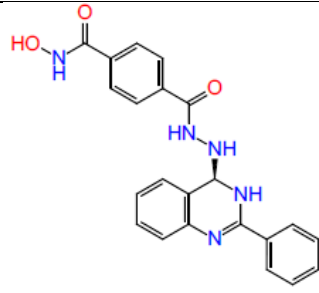
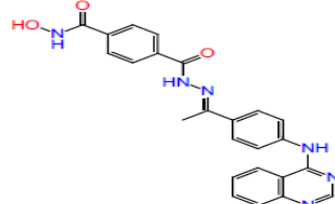
METHODOLOGY

PV38		-7.469	-9.706
PV39		-9.541	-9.360
PV40		-10.676	-8.840
PV41		-6.852	-8.267
PV42		-6.569	-9.042
PV43		-7.783	-6.897

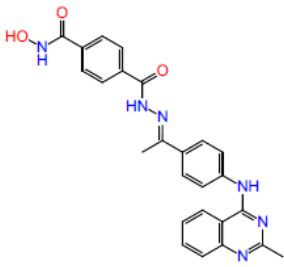
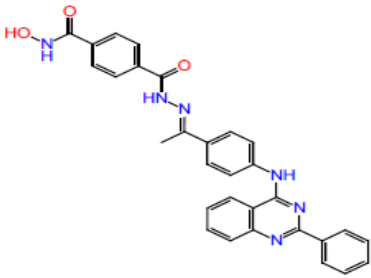
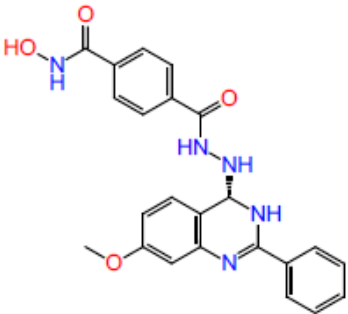
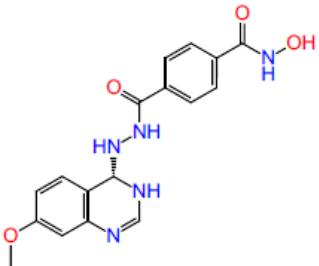
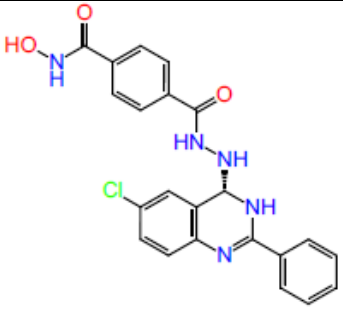
METHODOLOGY

PV44		-6.821	-10.563
PV45		-6.815	-8.326
PV46		-5.833	-8.446
PV47		-6.612	-8.391
PV48		-6.780	-8.918
PV49		-8.085	-9.190

METHODOLOGY

PV50		-8.260	-8.984
PV51		-7.491	-8.806
PV52		-9.172	-9.734
PV53		-4.305	-4.305
PV54		-6.402	-6.402
PV55		-7.995	-8.047

METHODOLOGY

PV56		-6.733	-6.741
PV57		-9.246	-9.042
PV58		-7.486	-9.887
PV59		-8.611	-9.780
PV60		-7.232	-9.286

Validation of Docking Protocol:

Validation of docking protocol was done by redocking.

Ligand interaction with receptor

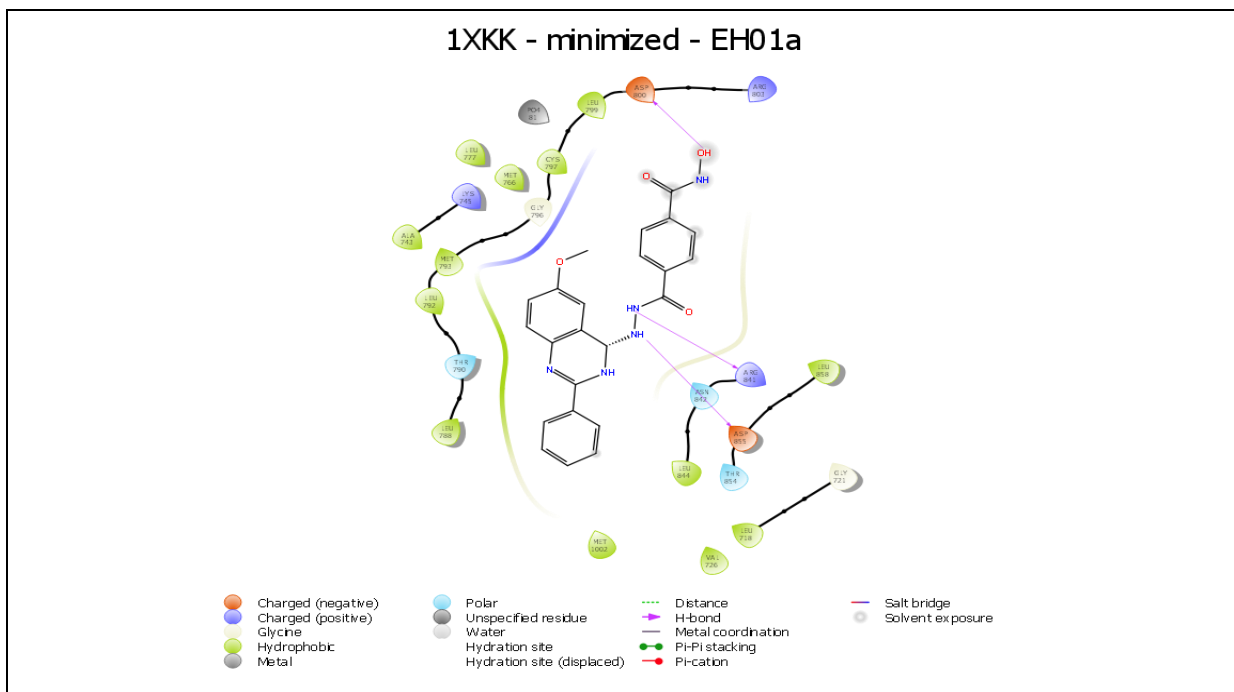


Fig: 6 - 2D docked conformer of EH01 with EGFR (1XKK)

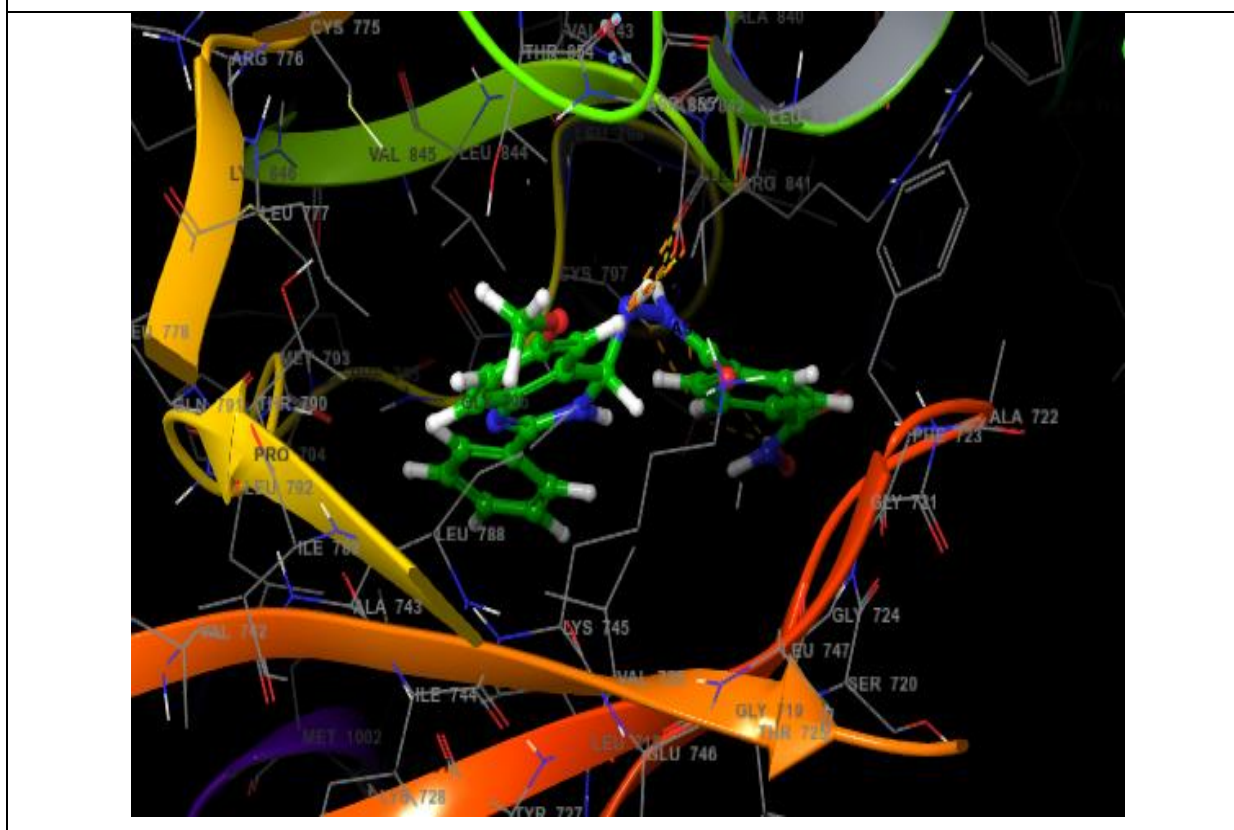


Fig: 7 - 3D docked conformer of EH01 with EGFR (1XKK)

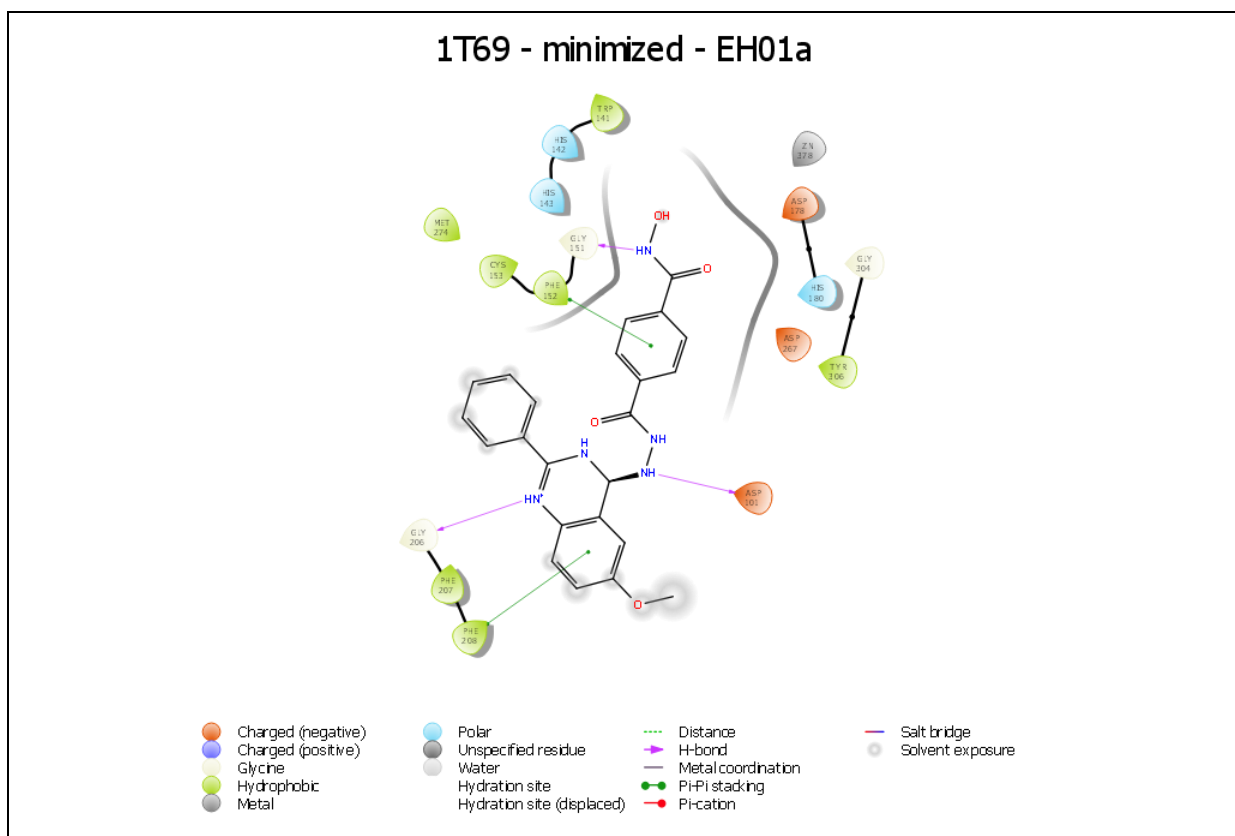


Fig: 8 - 2D docked conformer of EH01 with HDAC (1T69)

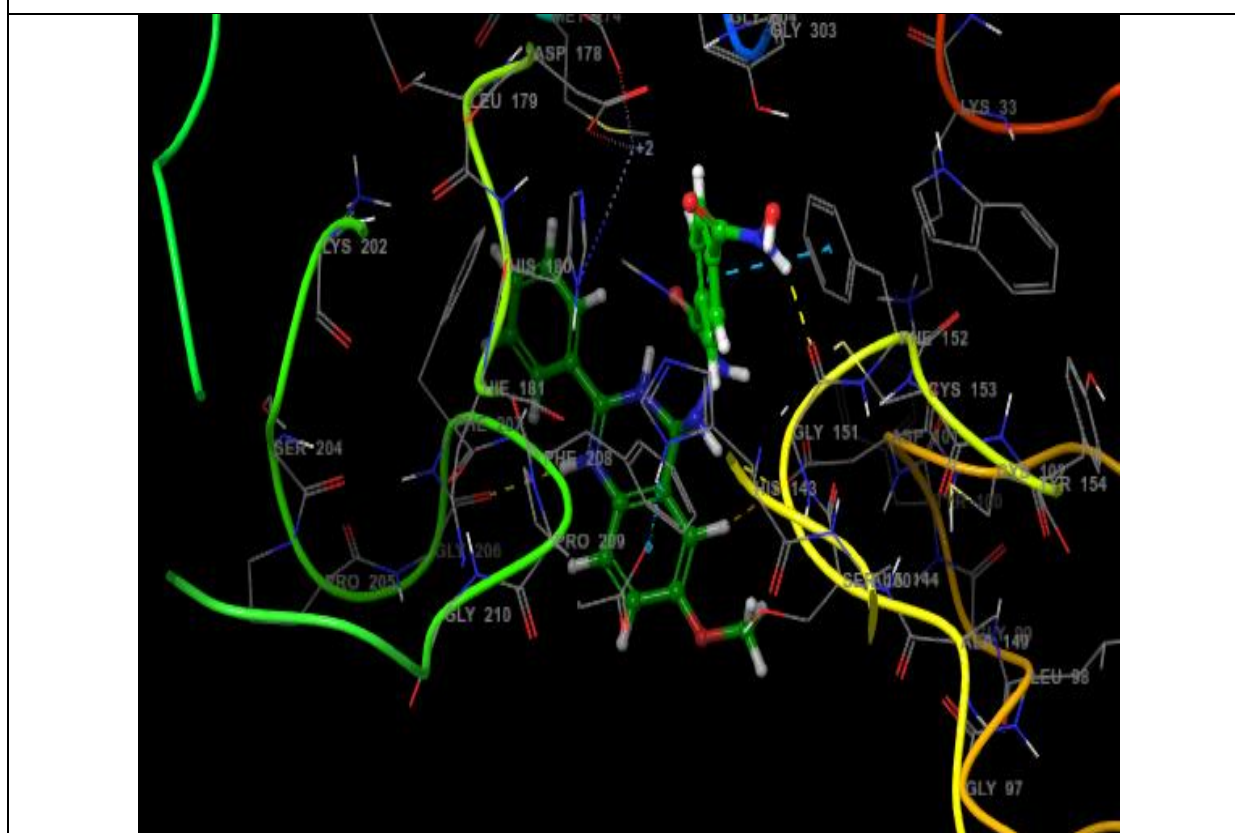


Fig: 9 - 3D docked conformer of EH01 with HDAC (1T69)

1XKK - minimized - EH 02

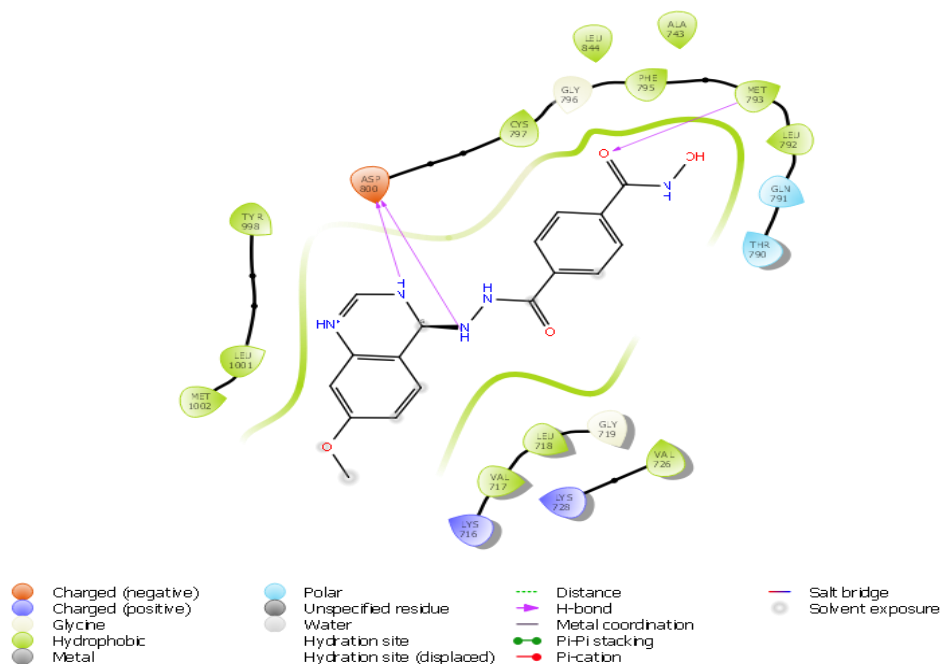


Fig: 10 - 2D docked conformer of EH02 with EGFR (1XKK)

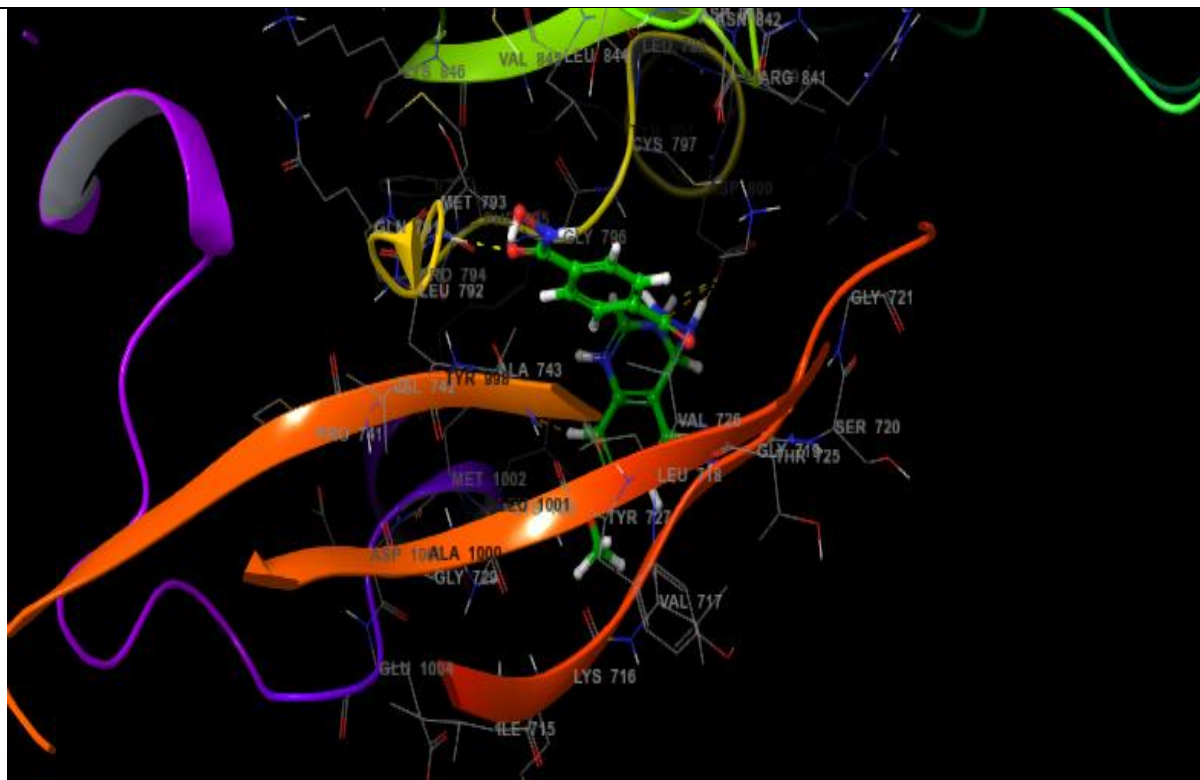


Fig: 11 - 3D docked conformer of EH02 with EGFR (1XKK)

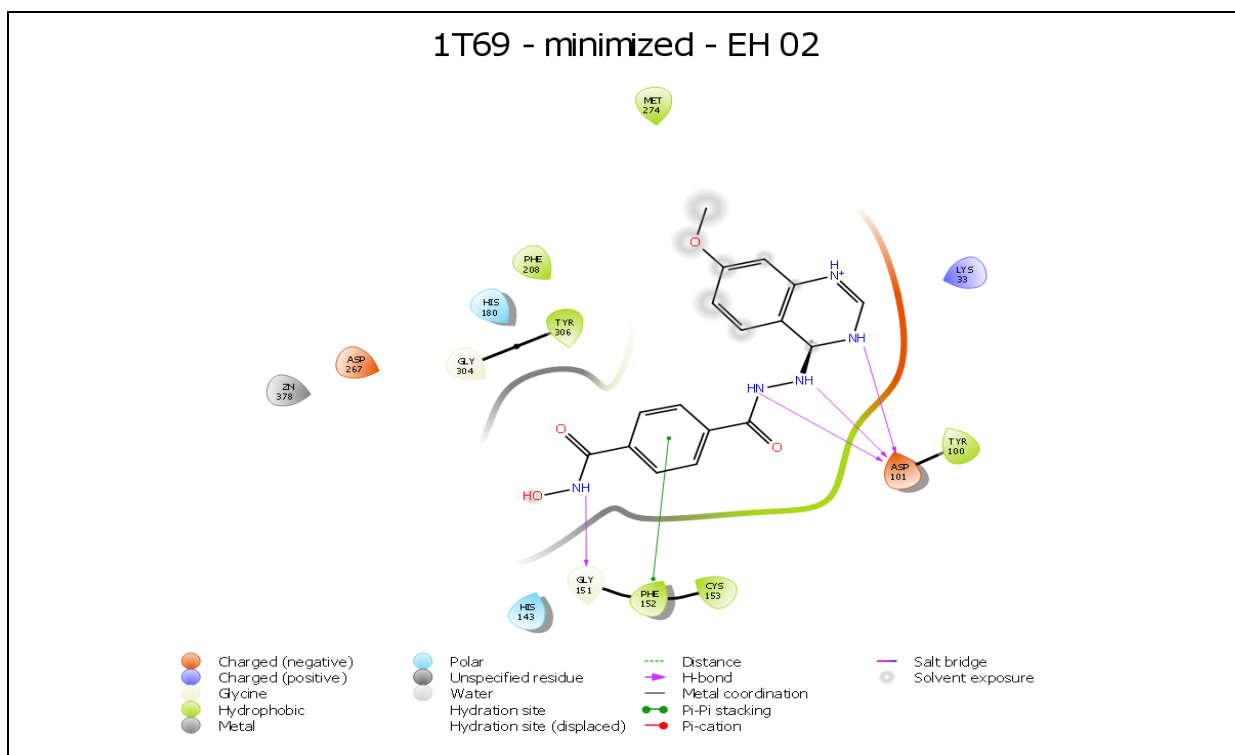


Fig: 12 - 2D docked conformer of EH02 with HDAC (1T69)

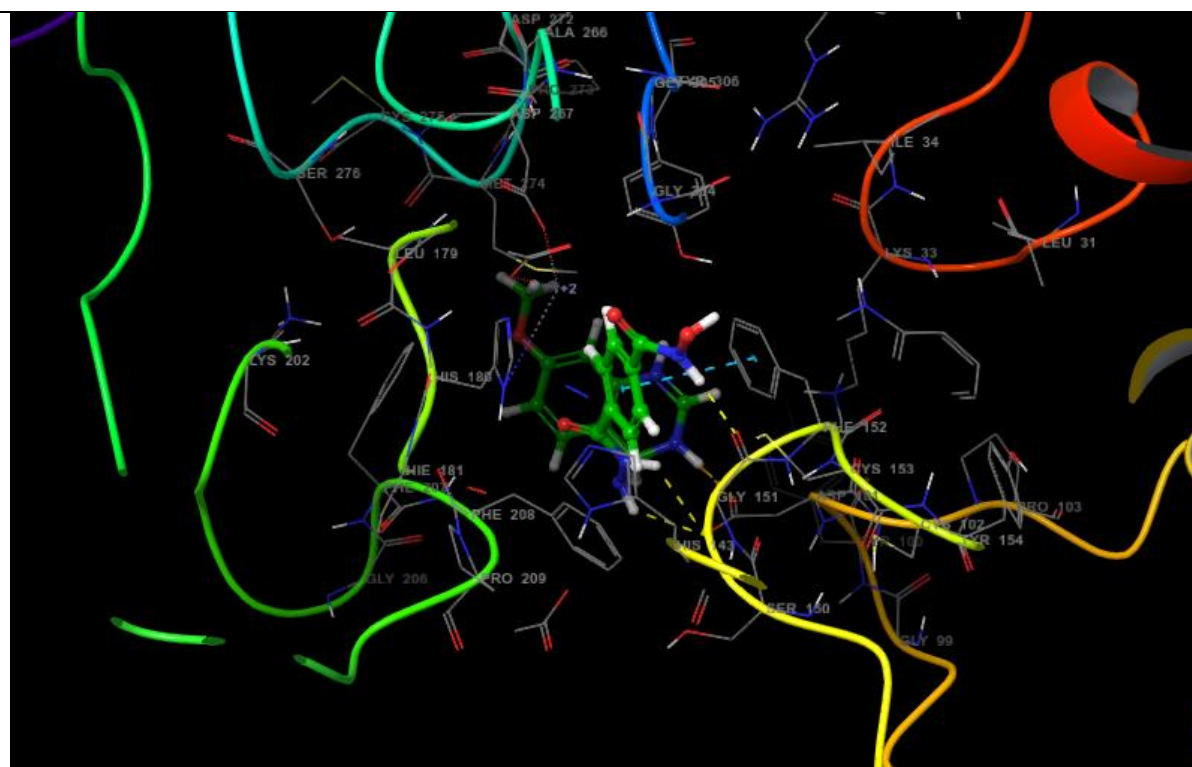


Fig: 13 - 3D docked conformer of EH02 with HDAC (1T69)

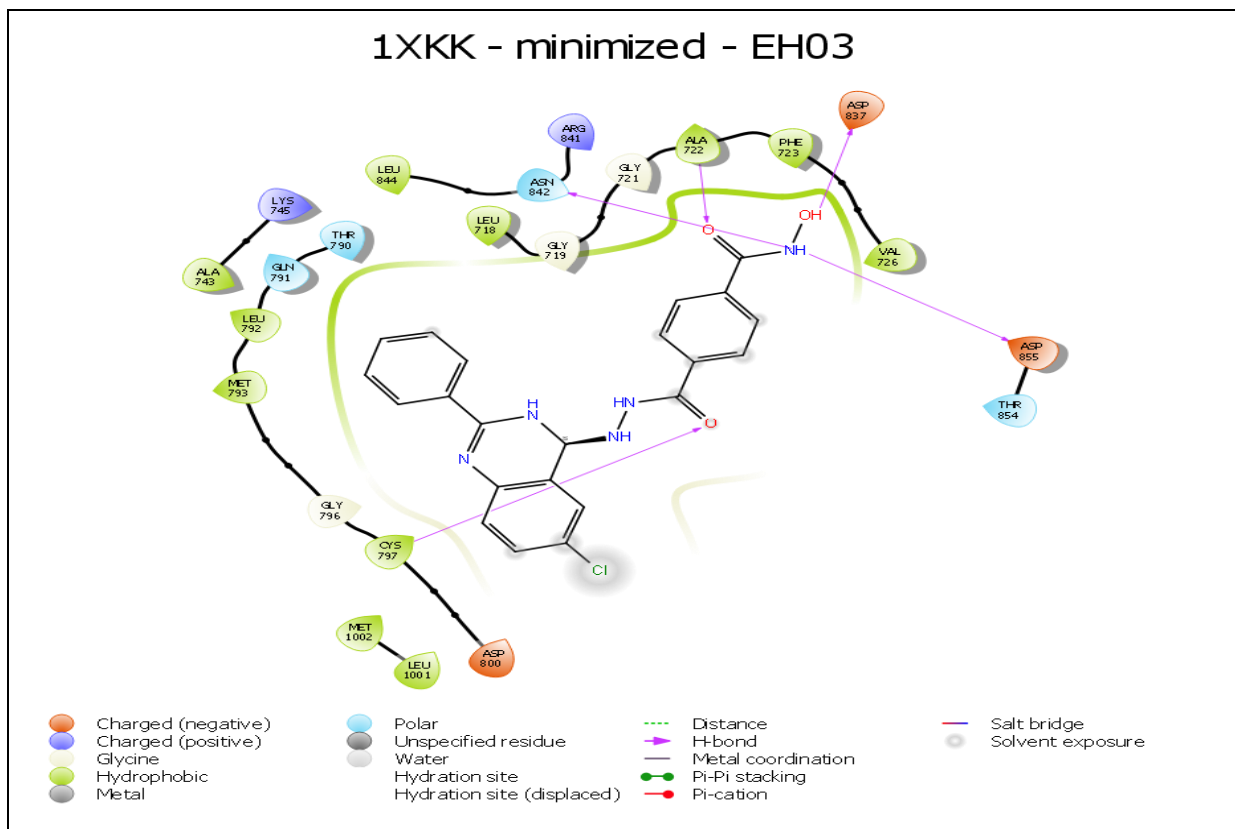


Fig: 14 - 2D docked conformer of EH03 with EGFR (1XKK)

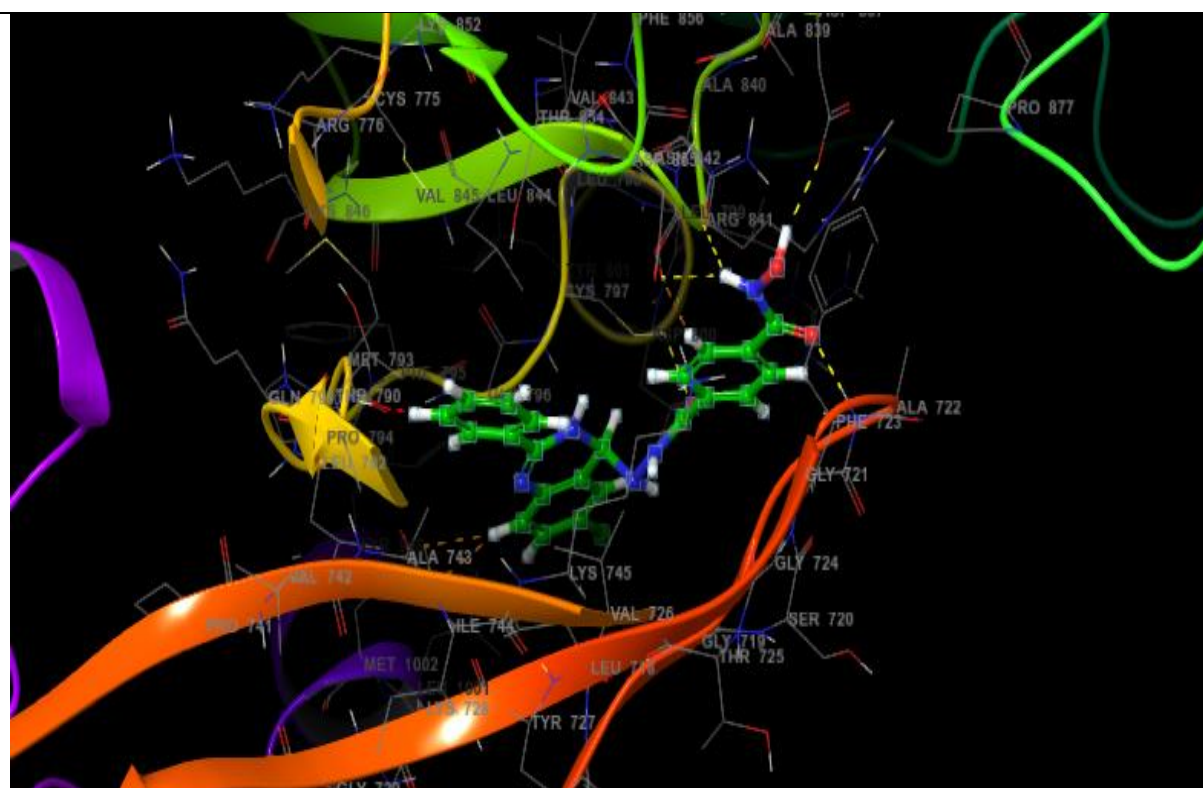


Fig: 15 - 3D docked conformer of EH03 with EGFR (1XKK)

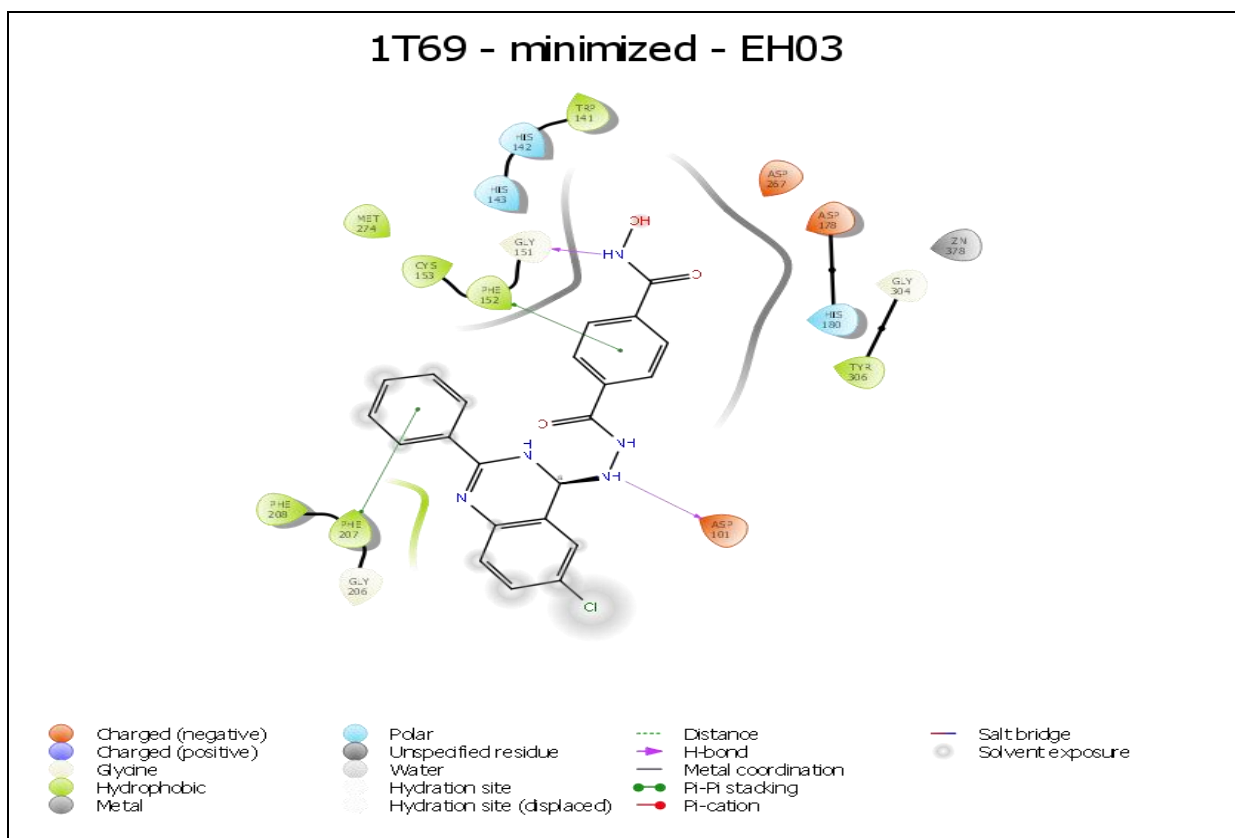


Fig: 16 - 2D docked conformer of EH03 with HDAC (1T69)

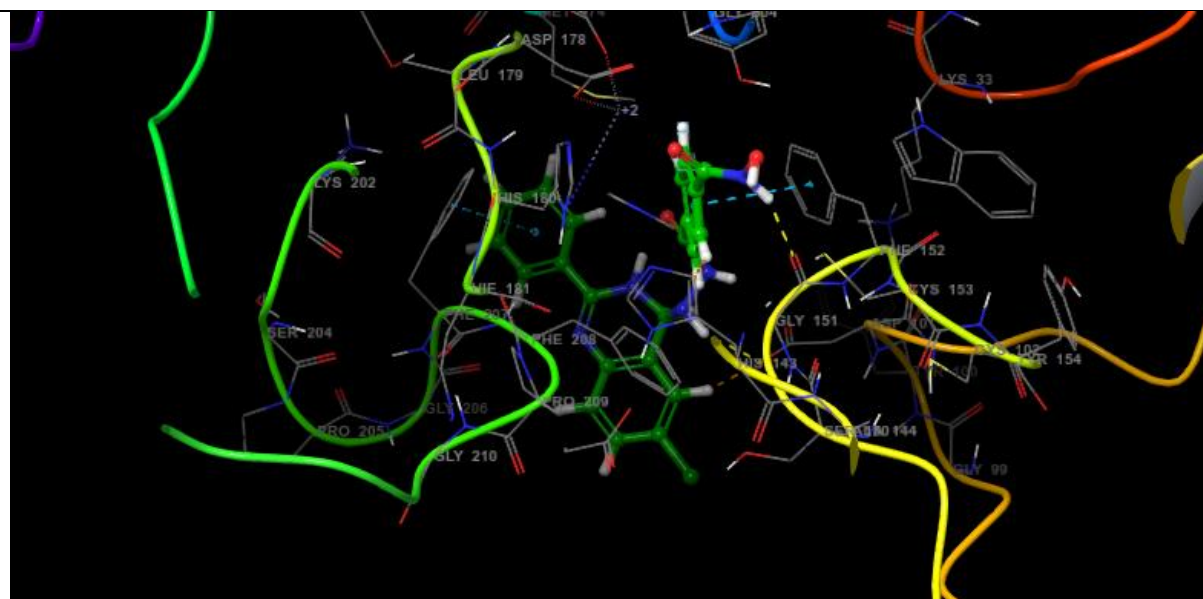
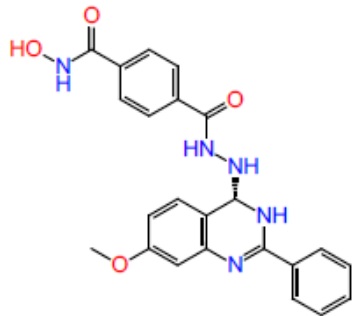
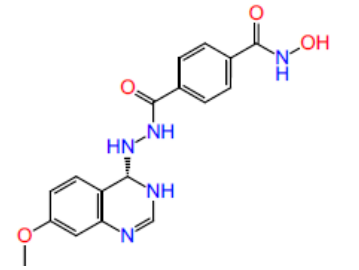
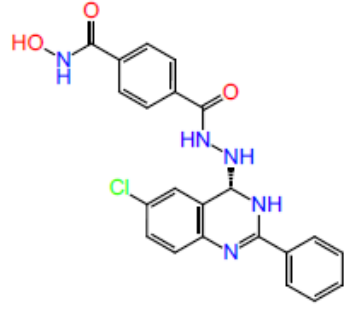


Fig: 17 - 3D docked conformer of EH03 with HDAC (1T69)

Table: 3 Ligands and their interaction with binding sites

S.no	Code	Structure	Interaction (EGFR: 1XKK)	Interaction (HDAC:1T69)
1	EH01		- 3H bond with Asp 800, ARG 811 and ASP 855	- 3H bond with ASP 101, GLY 151 and GLY 206 - 2 pi-pi stacking with PHE 152 and PHE 208
2	EH02		-3H bond with ASP 100 and MET 793	- 4 H bond with GLY 151 and ASP 101. - 1 pi-pi stacking with PHE 152
3	EH03		- 5H bond with CYS 797, ALA 722, ASP 837 and 855, ASN 942.	- 2H bond with ASP 101 and GLY 151 - 2 pi-pi stacking with PHE 152 and 207.

Prediction of ADME properties:

Most of drug candidates fail in clinical trials due to poor ADME properties. Thus, an important aspect of drug discovery is to avoid compounds not having drug likeliness and good ADME property. Drug likeliness and ADME properties of all the compounds were predicted using QikProp, version 4.5 of Schrodinger 2015. QikProp is quick accurate, easy to use absorption, metabolism and excretion (ADME) prediction program. Qikprop predicts physically significant descriptors and pharmaceutically relevant properties of organic molecules, either individually or in batches. In addition to predicting molecular properties, Qikprop provides ranges of

comparing particular molecules properties with those of 95% of known drugs. It also analyses the accept ability or suitability of compounds by applying the principles of Lipinski's rule of five, which is essential in drug design. The predicted properties include molecular weight, hydrogen bond donors and acceptors, QPlogHERG, QPPCaco, QPlogBB, CNS.

The designed molecules structure were created as 3D and prepared with LigPrep tool in mastero. The prepared Ligands were ran with Fast Mode default analysis in QikProp tool.

Table:4 Qikprop Results of designed ligands

CODE	M.WT (< 500)	HYDROGEN BOND DONOR (<5)	HYDROGEN BOND ACCEPTOR (< 10)	QPlogP (8 - 35)	Rule of Five (max 4)	Percentage Oral absorption (> 80 High < 25 poor)	QPPCaco (<25 poor >500 great)	QPlogBB (-3 to -1.2)	QPPMDCK (<25 poor >500 great)	QPlogKhsa (- 1.5 to 1.5)	QPlogHERG (below -5)	QPlogS (-6.5 to 0.5)	PSA (7 - 200)	#rotor (0-15)
PV1	463.495	4	9.45	27.603	1	44.635	19.062	-2.599	25.325	-0.495	-4.24	-3.788	157.975	8
PV2	360.372	4	9.59	23.422	0	47.801	26.649	-1.881	36.194	-1.104	-2.536	-1.411	147.776	5
PV3	477.522	4	8.7	27.596	1	50.589	26.038	-2.389	35.478	-0.258	-3.904	-4.15	152.353	8
PV4	330.346	4	9.2	22.676	0	47.535	26.648	-1.78	36.194	-1.093	-2.688	-1.281	139.293	4
PV5	467.914	4	8.7	27.503	0	59.695	19.04	-2.376	54.935	-0.405	-4.32	-4.208	149.51	7
PV6	359.384	4	10.45	23.198	0	57.923	65.929	-1.698	51.262	-0.876	-3.578	-1.937	138.209	6
PV7	492.533	4	10.7	27.984	1	55.75	53.207	-2.416	40.604	-0.325	-5.155	-4.284	156.597	10
PV8	493.521	4	10.2	28.233	1	46.024	21.601	-2.624	28.991	-0.51	-4.05	-3.882	163.985	9
PV9	479.556	4	11.45	28.552	0	71.248	77.431	-2.034	119.607	-0.437	-5.595	-4.666	139.035	8
PV10	480.543	4	10.95	28.575	1	57.839	66.713	-2.1	100.65	-0.327	-5.705	-5.091	143.831	7
PV11	512.542	6	13.2	34.377	3	0	0.779	-4.414	0.948	-1.076	-4.373	-2.801	214.539	9
PV12	497.94	4	9.45	28.657	1	41.26	8.807	-2.857	35.486	-0.357	-4.444	-4.26	155.852	8
PV13	497.94	4	9.45	28.178	1	48.72	22.239	-2.392	67.966	-0.402	-4.145	-4.408	156.823	8
PV14	491.505	3	10.45	28.794	1	26.6222	2.263	-3.823	4.111	-0.466	-4.61	-3.678	186.834	9
PV15	477.522	4	9.45	27.75	1	50.124	28.941	-2.564	34.397	-0.425	-4.372	-4.319	152.643	9
PV16	532.385	4	9.45	29.159	2	32.8	11.085	-2.619	86.44	-0.267	-4.367	-4.758	154.106	8
PV17	493.521	4	10.2	28.178	1	45.927	21.601	-2.63	28.991	-0.517	-4.064	-3.882	163.985	9
PV18	470.53	4	11.45	28.742	1	19.968	2.101	-2.497	4.05	-0.706	-4.412	-1.766	170.798	8
PV19	452.472	5	9.45	28.304	0	35.43	9.964	-2.914	12.666	-0.663	-3.934	-3.325	173.42	8
PV20	479.556	4	11.45	28.613	0	71.411	75.898	-2.1	116.607	-0.421	-5.736	-4.897	139.1	8

METHODOLOGY

PV21	479.494	5	10.2	29.566	1	32.735	7.157	-3.171	8.785	-0.683	-4.047	-3.368	177.13	9
PV22	456.460	4	9.950	20.124	0	73.322	61.444	-2.753	24.257	-0.018	-7.849	-5.716	154.157	9
PV23	490.905	4	9.950	28.469	0	77.405	72.967	-2.753	61.150	0.070	-7.760	-6.372	152.356	9
PV24	472.459	4	9.700	28.287	1	53.407	26.770	-3.283	9.881	0.025	-7.744	-5.831	173.590	10
PV25	471.474	5	9.950	29.727	2	37.677	23.107	-3.371	8.428	-0.061	-7.743	-5.917	176.999	10
PV26	472.520	4	10.950	28.434	0	82.692	157.537	-2.101	150.698	-0.106	-7.872	-6.024	134.436	9
PV27	323.310	4	9.700	22.979	0	60.992	27.909	-2.001	27.909	-0.613	-6.217	-3.180	137.457	5
PV28	357.755	4	9.700	23.633	0	64.720	78.713	-1.885	66.763	-0.542	-6.344	-3.849	136.583	5
PV29	338.325	5	9.700	24.688	1	38.934	27.989	-2.487	10.369	-0.633	-6.079	-3.261	158.967	6
PV30	339.310	4	9.450	23.264	0	54.081	31.464	-2.430	11.767	-0.596	-6.080	-3.149	155.788	6
PV31	353.337	4	10.450	23.725	0	61.235	69.956	-2.101	27.909	-0.628	-6.054	-3.301	145.939	6
PV32	501.457	4	10.950	30.053	2	31.997	12.569	-3.747	4.364	-0.068	-7.778	-5.866	194.618	10
PV33	486.547	4	10.950	28.939	0	82.834	130.409	-2.371	117.900	-0.018	-8.067	-6.507	135.563	10
PV34	367.363	4	10.450	24.256	0	63.387	69.956	-2.297	27.909	-0.562	-6.424	-3.789	145.421	7
PV35	353.337	4	9.700	23.346	0	64.620	85.461	-1.912	34.651	-0.519	-5.786	-3.219	142.468	6
PV36	399.408	4	9.700	26.377	0	69.244	69.956	-2.273	27.909	-0.222	-7.363	-4.726	137.457	6
PV37	367.363	4	11.400	24.776	0	61.474	69.956	-2.259	27.909	-0.681	-6.314	-3.504	145.652	7
PV38	383.363	4	11.200	24.430	0	61.393	69.956	-2.210	27.909	-0.651	-5.913	-3.421	154.129	7
PV39	289.293	4	9.700	21.024	0	48.673	33.410	-2.185	24.506	-1.128	-4.245	-1.460	139.640	7
PV40	305.354	4	9.200	20.783	0	60.730	84.095	-1.618	143.588	-1.020	-4.246	-1.969	118.548	7
PV41	426.434	4	9.200	27.182	0	70.578	49.754	-2.737	19.310	-0.031	-7.914	-5.500	147.656	8
PV42	502.531	4	9.200	30.426	1	71.338	80.109	-2.716	32.312	0.474	-8.969	-7.243	143.335	9
PV43	502.531	4	9.200	27.392	0	77.117	77.973	-2.596	31.381	0.092	-7.811	-5.871	152.666	9
PV44	484.470	4	11.200	31.676	1	32.273	2.164	-4.013	0.829	-0.329	-6.221	-5.790	195.158	10
PV45	460.879	4	9.200	27.828	0	72.977	49.704	-2.616	41.887	0.053	-7.808	-6.062	147.673	8
PV46	460.879	4	9.200	27.798	0	74.626	57.728	-2.554	48.156	0.066	-7.867	-6.126	146.782	8

METHODOLOGY

PV47	440.460	4	9.200	27.525	0	75.425	68.138	-2.643	27.126	0.106	-7.872	-6.059	146.253	8
PV48	367.363	4	10.450	24.009	0	66.339	129.889	-1.386	54.479	-0.505	-3.778	-2.262	146.452	6
PV49	429.434	4	10.450	26.709	0	75.998	180.113	-1.442	77.568	-0.270	-5.217	-3.137	142.740	6
PV50	337.337	4	9.700	23.392	0	64.843	88.698	-1.940	36.072	-0.508	-6.134	-3.593	136.054	2
PV51	353.337	4	9.700	23.346	0	64.620	88.698	-1.912	34.651	-0.519	-5.786	-3.219	142.468	2
PV52	395.374	4	11.700	26.254	0	56.186	37.129	-2.392	14.073	-0.596	-5.806	-3.332	169.479	3
PV53	460.879	4	9.200	27.828	0	72.977	49.704	-2.616	41.887	0.053	-7.808	-6.062	147.673	8
PV54	460.879	4	9.200	27.798	0	74.626	57.728	-2.554	48.156	0.066	-7.867	-6.126	146.782	8
PV55	440.460	4	9.200	27.525	0	75.425	68.138	-2.643	27.126	0.106	-7.872	-6.059	146.253	8
PV56	470.53	4	11.45	28.742	1	19.968	2.101	-2.497	4.05	-0.706	-4.412	-1.766	170.798	8
PV57	452.472	5	9.45	28.304	0	35.43	9.964	-2.914	12.666	-0.663	-3.934	-3.325	173.42	8
PV58	431.450	5	9.950	19.837	0	75.301	110.922	-2.026	45.933	-0.161	-6.769	-4.649	143.206	7
PV59	355.352	5	9.950	20.283	0	66.629	61.575	-2.146	24.313	-0.551	-5.931	-3.429	147.862	6
PV60	435.869	5	9.200	22.145	0	75.206	98.743	-1.857	97.773	-0.093	-6.816	-5.112	134.345	6

4.2 SYNTHESIS OF COMPOUNDS

PROCEDURE:

COMPOUND EH01

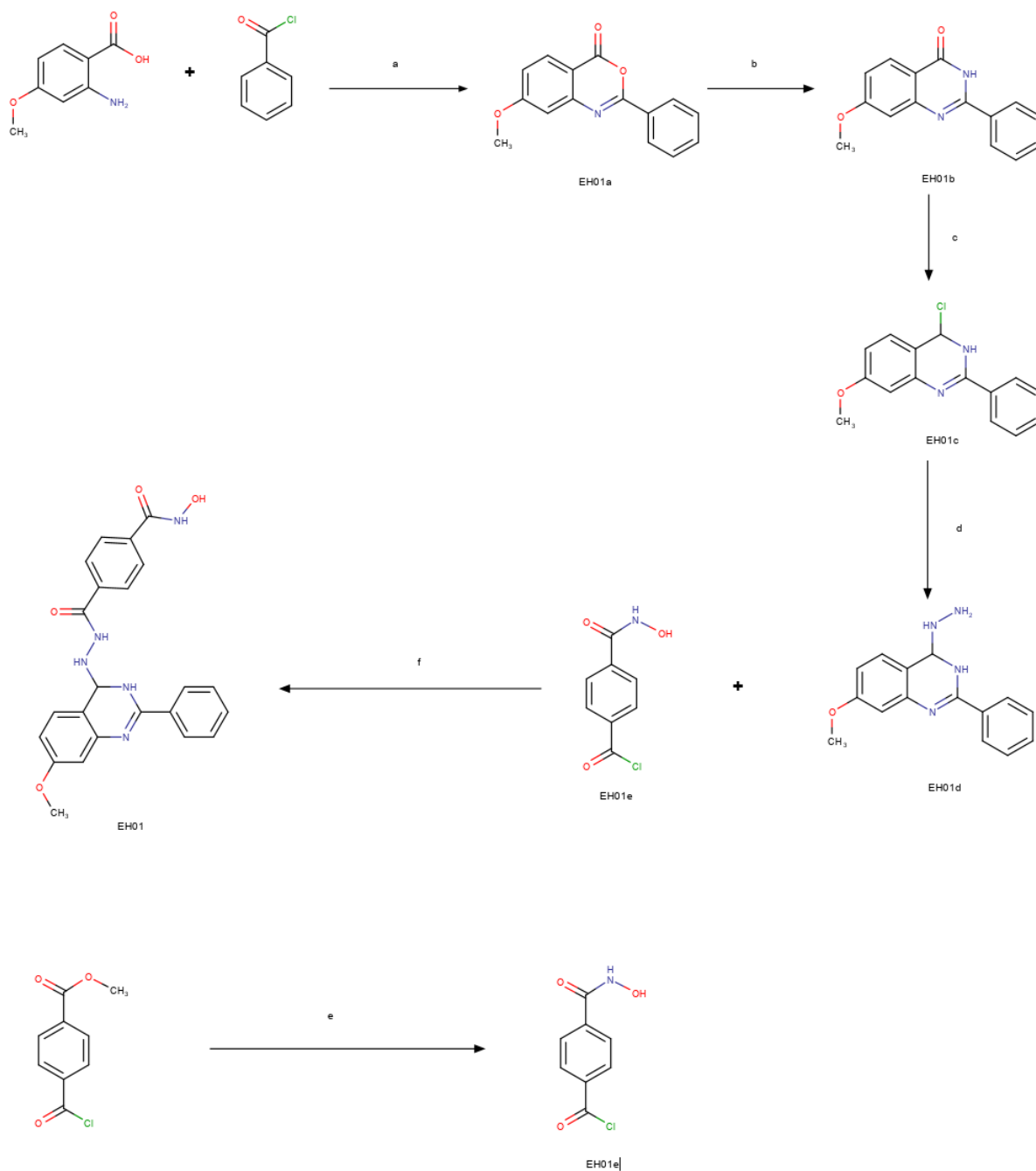


Fig:18 Synthesis Scheme of EH01

Step 1 Procedure for the synthesis of (7-methoxy) 2-(phenyl)-4Hbenz-(1,3)oxazine 4-one ^[35]

2-amino 5-chloro benzoic acid (1.716g) was dissolved in 20ml of anhydrous pyridine cooled to 0°C and added benzoyl chloride (2.32 ml) with continuous stirring for 30 minutes. After it was treated with 5% sodium bicarbonate to remove the unreacted acid till effervescence ceases, the obtained material was filtered. The product was dried to yield EH01a.

Step 2 Procedure for the synthesis of (7-methoxy) 2-(phenyl)-4Hbenz-(1,3)quinazoline 4-one ^[36]

To compound EH01a (39.5 μ mol) in pyridine equimolar quantity of ammonium acetate was added and refluxed under microwave irradiation for 5 mins at 425 watts. The mixture was then added to cold water. Allowed to stand for 1 hour and then filtered and dried to yield compound EH01b.

Step 3 Procedure for the synthesis of (7-methoxy) 2-(phenyl)-4chloro 4Hbenz-(1,3)quinazoline 4-one ^[37]

Compound EH01b (35.7 μmol) in thionyl chloride (2ml) containing DMF (10 μl) was refluxed under microwave irradiation for 6 mins at 340 watts. The mixture obtained was evaporated to get crude product of compound EH01c.

Step 4 Procedure for the synthesis of (7-methoxy) 2-(phenyl)-4hydrazino 4Hbenz-(1,3)quinazoline 4-one ^[38]

Compound EH01c was dissolved in 10ml ethanol and twice the mole of hydrazine hydrate and heated under microwave irradiation for 6 mins (425 watts – 4 mins and 570 watts – 2 mins) and cooled to room temperature and then evaporated to give compound EH01d

Step 5 Procedure for the synthesis of 4-(hydroxycarbamoyl)benzoyl chloride ^[39]

The compound EH01e was synthesized by dissolving methyl 4-[chlorocarbonyl] benzoate in dichloromethane and methanol in the ratio of 1:2 and then cooling the mixture to 0° C. When the mixture reached 0° C a mixture of

ammonium hydroxide and sodium hydroxide in methanol was added with stirring. Then the solution mixture is stirred for 2hrs continuously at 0° C and then filtered and dried.

Step 6 Procedure for the synthesis of N-hydroxy-4-[N'-(7-methoxy-2-phenyl-3,4-dihydroquinazolin-4-yl)hydrazinecarbonyl]benzamide ^[40]

The compounds EH01d in triethylamine was added to solution of EH01e in tetrahydrofuran at 0° C and stirred continuously for 4hrs to yield the compound EH01.

COMPOUND EH02

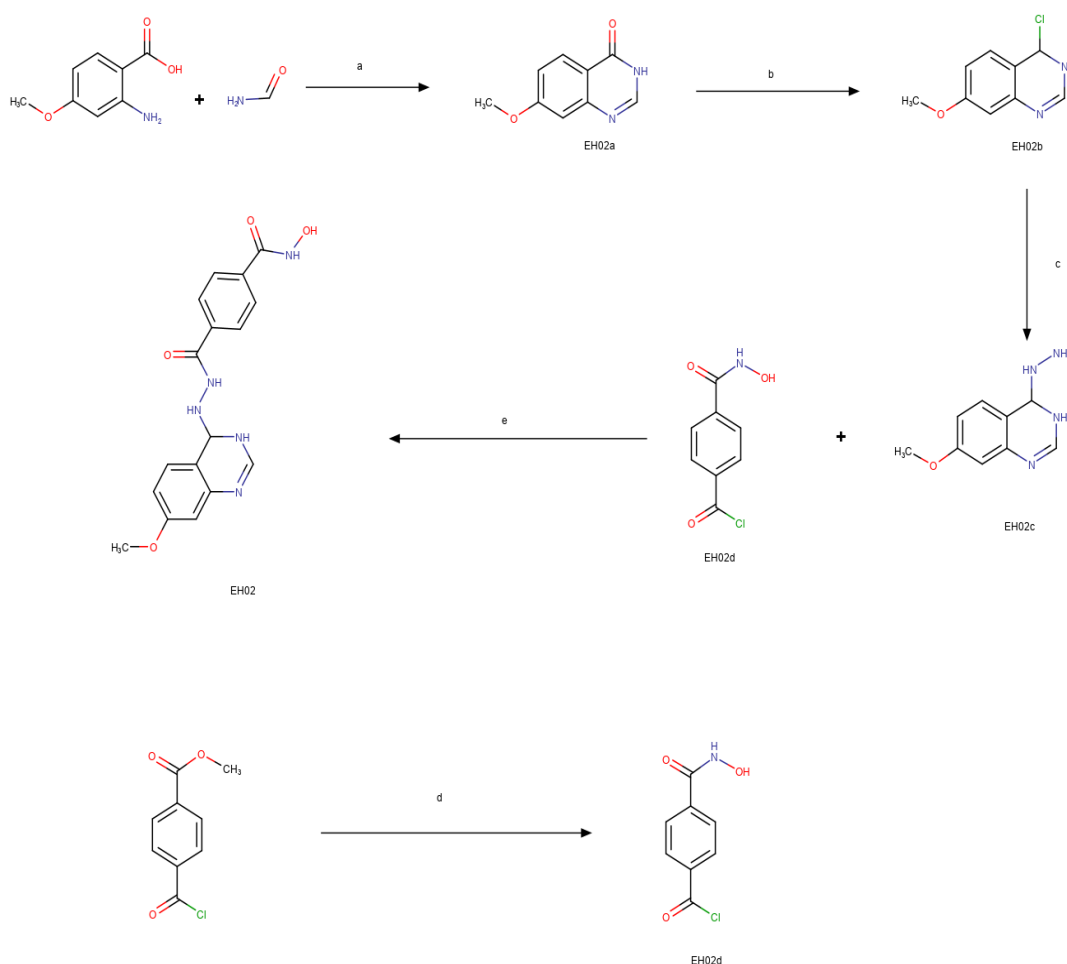


Fig:19 Synthesis Scheme of EH02

Step 1 Procedure for the synthesis of (7-methoxy)-4Hbenz-(1,3) quinazoline 4-one ^[35]

2-amino 4-methoxy benzoic acid was dissolved excess quantity of formamide and refluxed under microwave irradiation for 6 mins at 340 watts. The solution was then cooled and filtered. The product was dried to yield EH02a.

Step 2 Procedure for the synthesis of (7-methoxy) 4chloro 4Hbenz-(1,3) quinazoline 4-one ^[36]

Compound EH02a (35.7 μ mol) in thionyl chloride (2ml) containing DMF (10 μ l) was refluxed under microwave irradiation for 6 mins at 340 watts. The mixture obtained was evaporated to get crude product of compound EH02b.

Step 3 Procedure for the synthesis of (7-methoxy) 4hydrazino 4Hbenz-(1,3) quinazoline 4-one ^[37]

Compound EH02b was dissolved in 10ml ethanol and twice the mole of hydrazine hydrate and heated under microwave irradiation for 6 mins (425 watts – 4 mins and 570 watts – 2 mins) and cooled to room temperature and then evaporated to give compound EH02c

Step 4 Procedure for the synthesis of 4-(hydroxycarbamoyl)benzoyl chloride ^[38]

The compound EH02d was synthesized by dissolving methyl 4-[chlorocarbonyl] benzoate in dichloromethane and methanol in the ratio of 1:2 and then cooling the mixture to 0°C. When the mixture reached 0° C a mixture of ammonium hydroxide and sodium hydroxide in methanol was added with stirring. Then the solution mixture is stirred for 2hrs continuously at 0° C and then filtered and dried.

Step 5 Procedure for the synthesis of N-hydroxy-4-[N'-(7-methoxy-3,4-dihydroquinazolin-4-yl)hydrazinecarbonyl]benzamide ^[39]

The compounds EH02c in triethylamine was added to solution of EH02d in tetrahydrofuran at 0° C and stirred continuously for 4hrs to yield the compound EH02

COMPOUND EH03

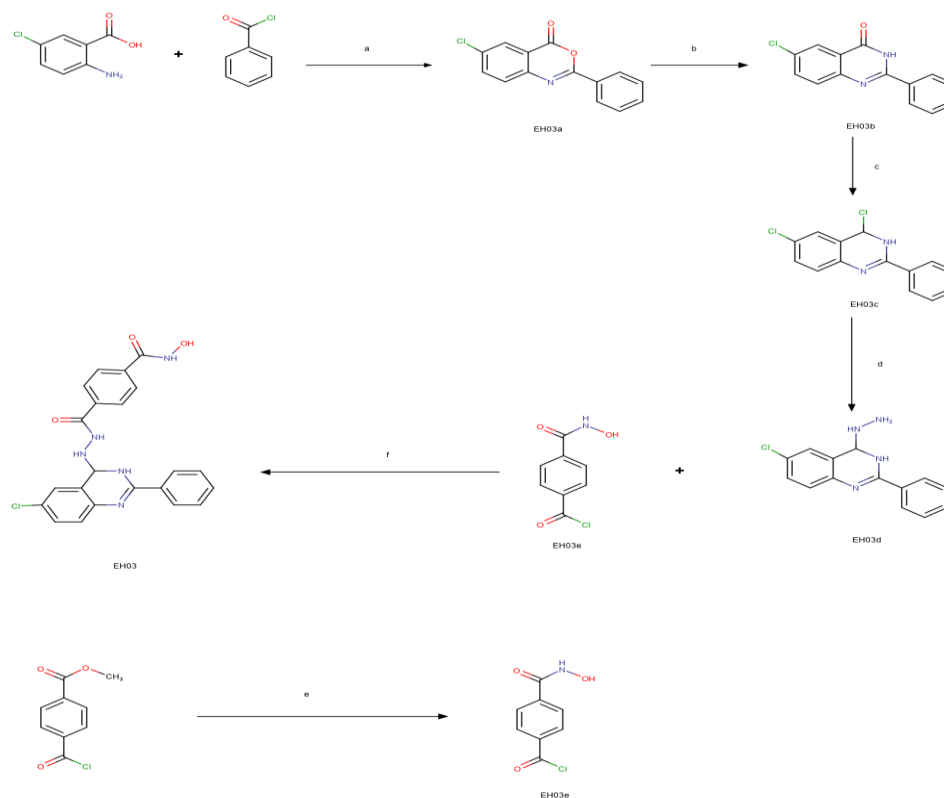


Fig:20 Synthesis Scheme of EH03

Step 1 Procedure for the synthesis of (6-chloro) 2-(phenyl)-4Hbenz-(1,3)oxazine 4-one^[35]

2-amino 5-chloro benzoic acid (1.716g) was dissolved in 20ml of anhydrous pyridine cooled to 0°C and added benzoyl chloride (2.32 ml) with continuous stirring for 30 minutes. After it was treated with 5% sodium bicarbonate to remove the unreacted acid till effervescence ceases, the obtained material was filtered. The product was dried to yield EH03a.

Step 2 Procedure for the synthesis of (6-chloro) 2-(phenyl)-4Hbenz-(1,3)quinazoline 4-one^[36]

To compound EH03a (39.5μ mol) in pyridine equimolar quantity of ammonium acetate was added and refluxed under microwave irradiation for 5 mins at 425 watts. The mixture was then added to cold water. Allowed to stand for 1hour and then filtered and dried to yield compound EH03b.

Step 3 Procedure for the synthesis of (6-chloro) 2-(phenyl)-4chloro 4Hbenz-(1,3) quinazoline 4-one ^[37]

Compound EH03b (35.7 μ mol) in thionyl chloride (2ml) containing DMF (10 μ l) was refluxed under microwave irradiation for 6 mins at 340 watts. The mixture obtained was evaporated to get crude product of compound EH03c.

Step 4 Procedure for the synthesis of (6-chloro) 2-(phenyl)-4hydrazino 4Hbenz-(1,3) quinazoline 4-one ^[38]

Compound EH03c was dissolved in 10ml ethanol and twice the mole of hydrazine hydrate and heated under microwave irradiation for 6 mins (425 watts – 4 mins and 570 watts – 2 mins) and cooled to room temperature and then evaporated to give compound EH03d

Step 5 Procedure for the synthesis of 4-(hydroxycarbonyl) benzoyl chloride ^[39]

The compound EH03e was synthesized by dissolving methyl 4-[chlorocarbonyl] benzoate in dichloromethane and methanol in the ratio of 1:2 and then cooling the mixture to 0°C. When the mixture reached 0° C a mixture of ammonium hydroxide and sodium hydroxide in methanol was added with stirring. Then the solution mixture is stirred for 2hrs continuously at 0° C and then filtered and dried.

Step 6 Procedure for the synthesis of N-hydroxy-4-[N'-(6-chloro-2-phenyl-3,4-dihydroquinazolin-4-yl)hydrazinocarbonyl]benzamide ^[40]

The compounds EH03d in triethylamine was added to solution of EH03e in tetrahydrofuran at 0° C and stirred continuously for 4hrs to yield the compound EH03

4.3 CHARACTERIZATION OF SYNTHESIZED COMPOUNDS

4.3.1 Physiochemical analysis

Physical parameters like percentage yield, molecular weight, molecular formula, melting point, logP and Rf value of the synthesized compounds were

determined and is given in **table**. The final compounds were in moderate to higher yields. The percentage yield was found to be in the range of 15 – 90%.

4.3.1.1 Melting point

Melting point has to be determined in open capillary tubes with electro thermal melting point apparatus.

4.3.1.2 Solubility

The solubility of all the compounds should be tested by using methanol, ethanol, chloroform, Dimethyl formamide, Dimethyl sulfoxide and water.

4.3.1.3 Thin Layer Chromatography

Thin layer chromatography is a method of analysis in which the stationary phase, a finely divided solid, is spread as a thin layer on a rigid supporting plate and the mobile phase, a liquid is allowed to migrate across the surfaces of the plate.

Applications of TLC

- To establish the purity and authenticity of starting material and reagents
- To monitor the reactions, particularly in the case of new reactions
- Assessment of purity of a crude reaction product
- The optimum of experimental conditions to achieve the highest possible yield of product

Provided that the experimental conditions are reproducible, the movement of any substance relative to the solvent front in a given chromatographic system is constant and characteristics of the substance. The constant is called as retention factor (R_f) and is defined as

$$R_f = \frac{\text{Distance travelled by solute}}{\text{Distance travelled by solvent front}}$$

True reproducibility in R_f value is, however, rarely achieved in practice due to minor changes in a number of variables such as:

1. The practical size of different batches of adsorbent
2. The solvent composition and the degree of saturation of the chamber atmosphere with solvent vapor.
3. Prior activation and storage conditions of the plate.
4. The thickness of adsorbent layer, etc.

It is therefore, not desirable to use R_f value in isolation as a criteria for identity.

TLC was performed using following procedure:

Dimension of plates	: 5*20cm
Stationary phase	: Silica gel- G 9E Merck
Mobile phase	: Chloroform : Ethanol (9:1)
Technique	: Ascending
Detection Method	: Iodine Chamber, Fluorescent Chamber

Preparation of Plates

Uniform slurry of Silica gel G was prepared by addition of distilled water. This was then poured into a spreading trough and drawn across a series of glass plates of size 5*20cm, depositing a uniform layer of stationary phase of 0.25mm thickness. The plates were air dried and then activated by heating at 110°C for one hour. The plates were stored over a dessicator until used.

Mobile Phase

Evaluation of various mobile phases was tried, alone or in combination for each compound in which Chloroform : Ethanol (9:1) was found to be suited.

Sample Application and Development

The samples were applied as small spot at about 2cm from the base of the plate. For ascending development of the thin layer chromatogram, the plate was placed in a TLC chamber, which was saturated with mobile phase containing the developing solvent to a depth of about 0.5cm. The solvent was allowed to move up the plate until it travelled a distance of about 15cm from the point of the sample, on a 20cm plate. The plate was then removed from the chamber, the solvent front was marked by scratching the surface and the plate was allowed to be evaporated.

Detection

After the chromatogram was developed the solute spots need to be made visible in order to determine their R_f values. Iodine chamber and fluorescent chamber were employed for the detection of the compounds by placing the plate in iodine chamber containing iodine crystals or fluorescent chamber. The solutes were visible as amber color spots.

Table: 5 Physical properties of synthesized compounds

S.No	Compound code	Molecular formula	Molecular weight (g)	Percentage yield (%)	Color	Melting point ($^{\circ}$ c)	R_f value*
1	EH 01a	$C_{15}H_{11}NO_3$	253.2522	17.76	White	210	0.77
	EH 01b	$C_{15}H_{12}N_2O_2$	252.267	90.91	White	198	0.56
	EH 01c	$C_{15}H_{13}N_2OCl$	272.7299	82.47	Yellow	232	0.72
	EH 01d	$C_{15}H_{16}N_4O$	268.3143	58.00	Brown	254	0.78
	EH 01	$C_{23}H_{20}N_5O_4$	430.4356	85.32	Brown	285	0.55
2	EH 02a	$C_9H_8N_2O_2$	176.1717	17.50	White	225	0.64
	EH 02b	$C_9H_8N_2OCl$	195.6257	79.91	Yellow	184	0.56
	EH 02c	$C_9H_{11}N_4O$	191.2101	82.47	Brown	245	0.80
	EH 02	$C_{17}H_{16}N_5O_4$	354.3394	78.42	Brown	287	0.75
3	EH 03a	$C_{14}H_8NO_2Cl$	257.6715	58.14	White	220	0.89
	EH 03b	$C_{14}H_9N_2OCl$	256.6872	26.10	White	208	0.74
	EH 03c	$C_{14}H_{10}N_2O_2Cl_2$	277.1492	87.26	Yellow	248	0.66
	EH 03d	$C_{14}H_{13}N_4Cl$	272.7336	43.88	Brown	262	0.75
	EH 03	$C_{22}H_{17}N_5O_3Cl$	434.855	82.58	Brown	255	0.69

4.3.2 Spectral analysis

4.3.2.1 Ultraviolet Spectrophotometry

Molecular absorption in the ultraviolet and visible region of the spectrum is dependent on the electronic structure of the molecule. Characteristic group with diverse electronic environment absorbs at selective wavelength and which helps in recognizing characteristic groups in a molecule of widely varying complexity.

UV spectra will be recorded on SHIMADZU 1700A spectrophotometer.

Table: 6 UV-vis spectral data of synthesized compounds

Code	λ_{max} (nm)	Absorbance
EH 01a	294	1.3412
EH 01b	262	0.5352
EH 01c	299.5	1.1456
EH 01d	278	2.598
EH 01	296	3.402
EH 02a	292	2.596
EH 02b	283	0.935
EH 02c	260	2.576
EH 02	295	2.486
EH 03a	274	1.452
EH 03b	295	2.546
EH 03c	262	3.999
EH 03d	282	3.999
EH 03	297	2.356

4.3.2.2 IR Spectroscopy

The range of electromagnetic radiation between 0.8 and 500 μm is referred as infrared radiation. An IR spectrum is commonly obtained by passing IR radiation through a sample and determining what fraction of the incident radiation is absorbed

at a particular energy. The energy at which any peak in an absorption spectrum appears corresponds to the frequency of a vibration of a part of a sample molecule.

Procedure: Pellet Technique

Solid samples should be intimately mixed with dry powdered potassium bromide. The mixture will then be pressed between a punch and disc under pressure of 1,00,000 – 15000 psi to form a transparent disc. The IR spectral study will be done on JASCO 4100 FTIR for the synthesized compounds to confirm their functional groups.

The spectral data showed the presence of functional groups in the synthesized compounds.

4.3.2.3 NMR Spectroscopy

NMR spectroscopy is an important tool for determining the structure of a molecule. NMR spectrum can give almost detailed information about molecular structure. NMR spectroscopy of the synthesized compounds has been done to confirm the molecular structure of the compounds. NMR spectrum can give almost unbelievably detailed information about molecular structure:

- a. The number of signals: which tell us how many different kinds of protons there are in a molecule
- b. The positions of the signals, which tell us something about the electronic environment of each kind of proton.
- c. The intensities of the signals, which tell us how many protons of each kind there are; and
- d. The splitting of a signal into several peaks, which tell us about the environment of a proton with respect to other, nearby protons.

NMR spectral study was done on Bruker Fourier, Transform-NMR Spectrometer on selected compound.

The spectral data for the prototype compound EH03 was given as follows.

Table: 7 NMR spectral data of Compound EH03

S.No	¹ H NMR (δ/ppm)
1	15.03 (s, 1H - NH - OH)
2	12.52 (s, 1H - NH - OH)
3	11.5 (s, 1H NH - C = O)
4	10.5 (s, 1H Ar - NH)
5	8.71 - 7.41 (m, 13H, Ar - H)

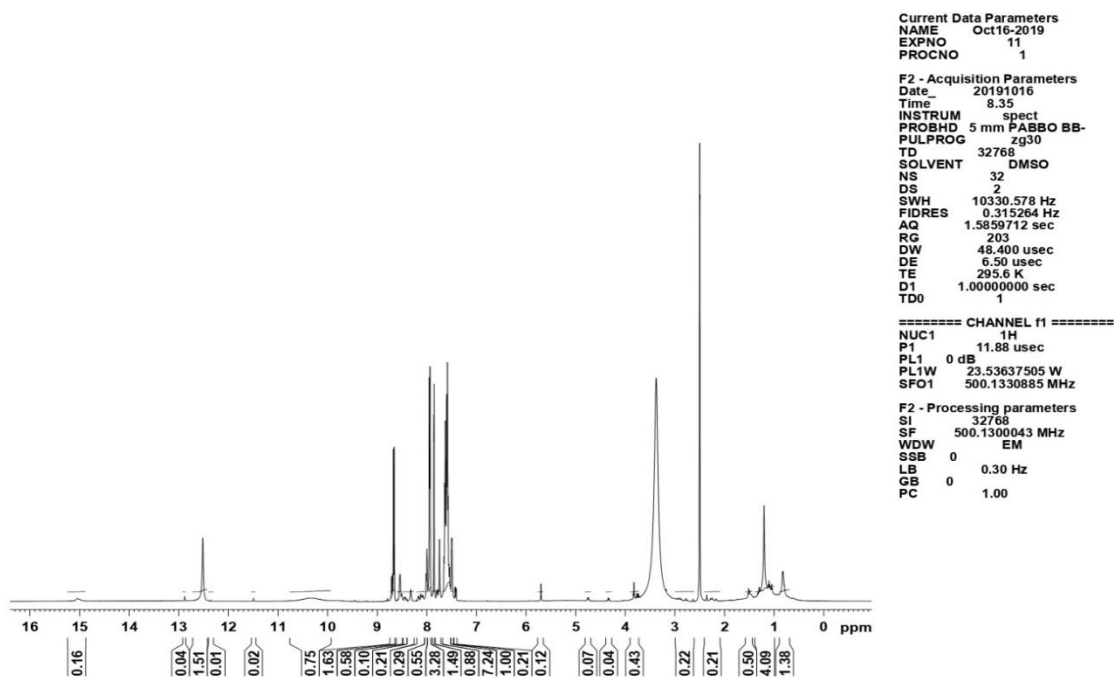


Fig: 21 NMR spectra of Compound EH 03

4.4 Cytotoxicity Study

MTT (3-(4,5-dimethylthiazol-2-yl)-2,5-diphenyl tetrazolium bromide) assay is a type of colorimetric assay which involves the measurement of the oxidoreductase enzyme activity in the cells which converts soluble dye MTT (yellow color) into

insoluble Formazan (purple color). It is used to determine the viability and proliferation of the cells. The cytotoxicity of the drugs or medicinal compounds can be determined using this study. Since, the anticancer drugs have to act on the cancerous cells and should inhibit its proliferation, the MTT assay is done for determining the cytotoxicity of the synthesized compounds. [41, 42]

Cell line

The MCF-7 cell line was obtained from National Centre for Cell Science (NCCS), Pune and grown in Eagles Minimum Essential Medium containing 10% fetal bovine serum (FBS). The cells were maintained at 37°C, 5% CO₂, 95% air and 100% relative humidity. Maintenance cultures were passaged weekly, and the culture medium was changed twice a week.

Cell treatment procedure

The monolayer cells were detached with trypsin-ethylenediaminetetraacetic acid (EDTA) to make single cell suspensions and viable cells were counted using a hemocytometer and diluted with medium containing 5% FBS to give final density of 1x10⁵ cells/ml. One hundred microlitres per well of cell suspension were seeded into 96-well plates at plating density of 10,000 cells/well and incubated to allow for cell attachment at 37°C, 5% CO₂, 95% air and 100% relative humidity. After 24 h the cells were treated with serial concentrations of the test samples. They were initially dissolved in dimethylsulfoxide (DMSO) by sonication and an aliquot of the sample solution was diluted to twice the desired final maximum test concentration with serum free medium. Additional four serial dilutions were made to provide a total of five sample concentrations. Aliquots of 100 µl of these different sample dilutions were added to the appropriate wells already containing 100 µl of medium, resulting in the required final sample concentrations. Following sample addition, the plates were incubated for an additional 48h at 37°C, 5% CO₂, 95% air and 100% relative humidity. The medium containing without samples were served as control and triplicate was maintained for all concentrations.

After 48 h of incubation, 15µl of MTT (5mg/ml) in phosphate buffered saline (PBS) was added to each well and incubated at 37°C for 4h. The medium with MTT

METHODOLOGY

was then flicked off and the formed formazan crystals were solubilized in 100µl of DMSO and then measured the absorbance at 570 nm using micro plate reader.

Con µg/ml	Absorbance		Percentage inhibition %
0	0.989	100	0
5	0.801	80.9909	19.0091
10	0.698	69.66633	30.33367
20	0.512	51.76946	48.23054
40	0.387	39.13043	60.86957
60	0.231	23.35693	76.64037
80	0.124	12.53792	87.46208

- The percentage cell growth was then calculated with respect to control as follows

$$\% \text{ Cell viability} = [A] \text{ Test} / [A] \text{ control} \times 100$$

Plot Non-linear regression graph between % Cell inhibition and \log_{10} concentration Determine IC_{50} using Graph Pad Prism software

In vitro anticancer activity of compound EH01 in MCF-7 cell line

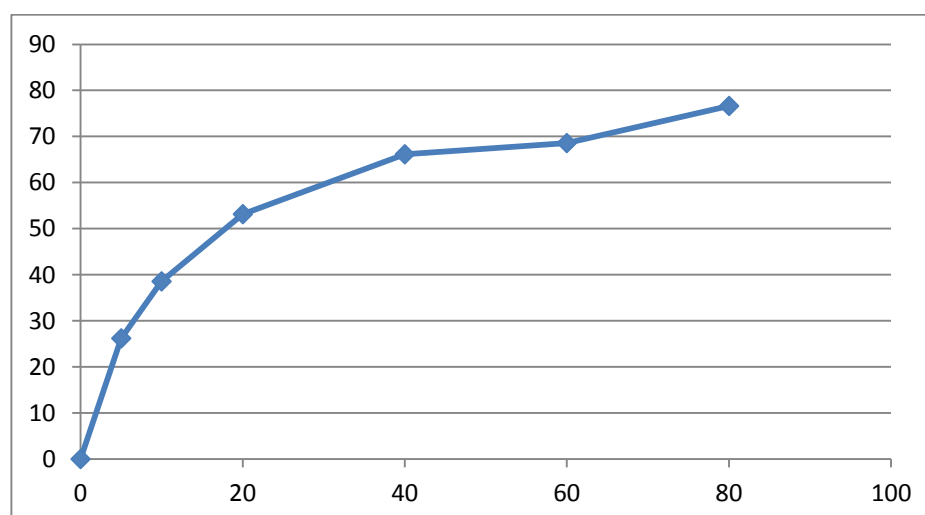


Fig: 22 Percentage inhibition of compound EH01

In vitro anticancer activity of compound EH02 in MCF-7 cell line

Con $\mu\text{g/ml}$	Absorbance		Percentage inhibition %
0	0.6935	100	0
5	0.512	73.828841	26.17159
10	0.426	61.42754	38.57246
20	0.325	46.86373	53.13627
40	0.235	33.8609	66.11391
60	0.218	31.43475	68.56525
80	0.162	23.35977	76.64023

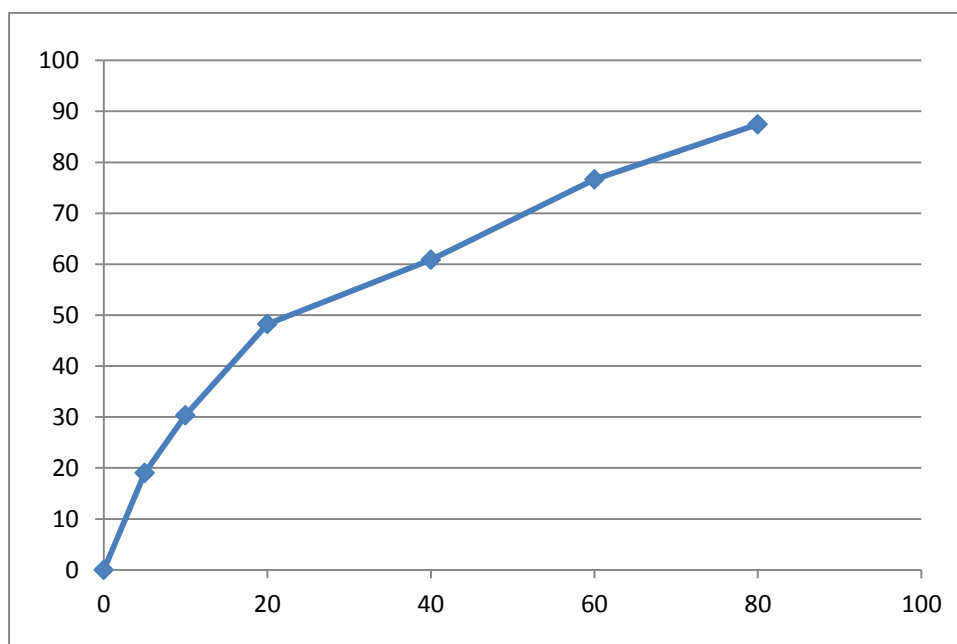


Fig: 23 Percentage inhibition of compound EH02

In vitro anticancer activity of compound EH03 in MCF-7 cell line

Con $\mu\text{g/ml}$	Absorbance		Percentage inhibition %
0	0.989	100	0
5	0.881	89.07988	10.92012
10	0.693	70.07078	29.92922
20	0.534	53.99393	46.00607
40	0.457	46.20829	53.79171
60	0.281	28.41254	71.58746
80	0.129	13.04348	86.95652

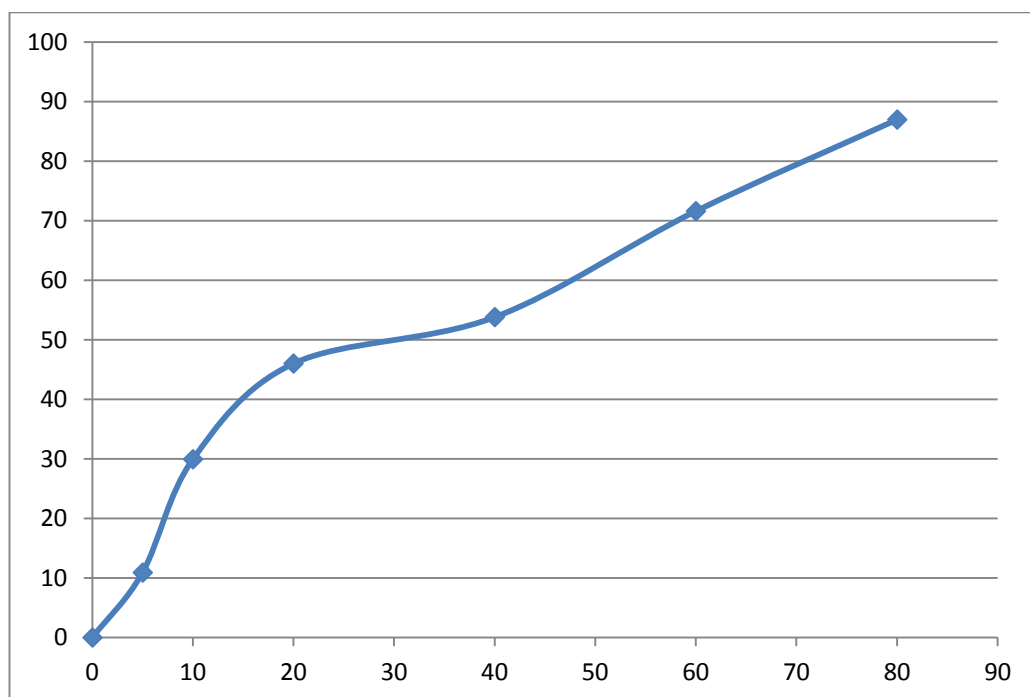
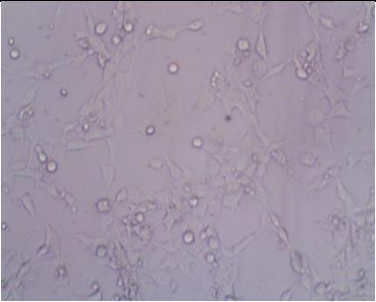
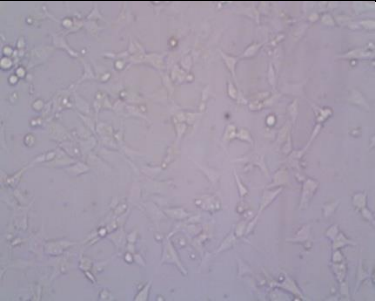
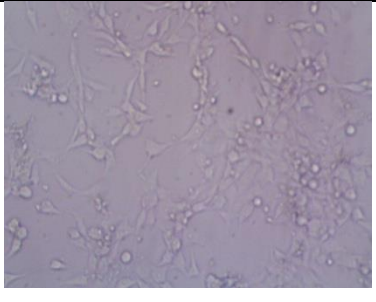
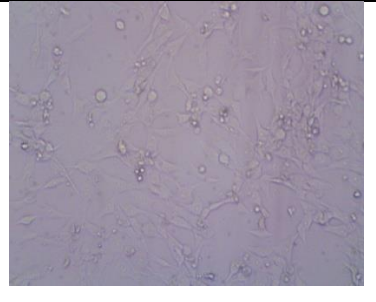
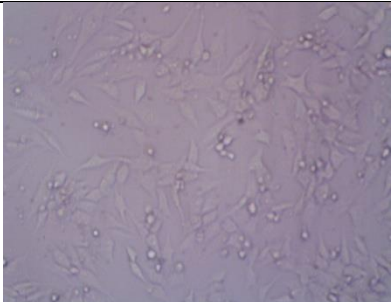
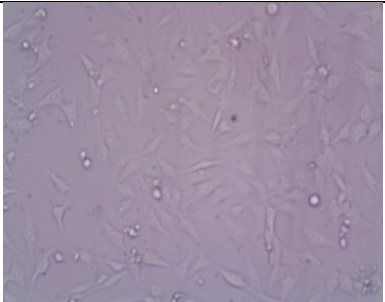


Fig: 24 Percentage inhibition of compound EH03

Fig: 25 % growth inhibition of Compound EH01

	
0 µg/ml	10 µg/ml
	
20 µg/ml	40 µg/ml
	
60 µg/ml	80 µg/ml

RESULT AND DISCUSSION

The EGFR and HDAC over-expression have been found to play a major role in cancer especially in mammary carcinoma condition. Thus inhibition of these targets may result in a compound with good anti-cancer activity against breast cancer. Multi targeted compound against both these two targets helps to improve efficacy of the compound. Hence, these two targets have been chosen as targets for designing dual inhibitor for breast cancer.

Docking Results:

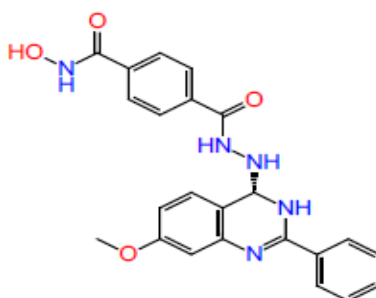
To investigate the binding modes, molecular docking of ligands against EGFR and HDAC proteins were performed using the GLIDE program (version 10.1, Schrodinger, LLC, NewYork 2015). To study interaction of ligands with targets the Maestro user interface (version 10.1 , Schrodinger, LLC, New York 2015) was employed to set up and execute the docking protocol and also for analysis of the docking results. Validation of docking protocol was done by re-docking.

Crystal structure of the targets have been selected from protein data bank based on certain criteria like resolution, method of preparation, etc., On docking studies it was observed that all the compounds bind at the active site of the targets with good affinity and had good interaction.

Amongst, PV58, PV59, PV60 was found with highest docking score and hydrogen bond interaction and pi-pi staking with the receptors.

RESULTS AND DISCUSSION

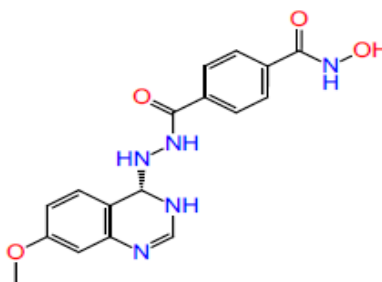
The compounds with their docking scores are as follows:



PV 58 [N-hydroxy-4-[N'-(7-methoxy-2-phenyl-3,4-dihydroquinazolin-4-yl)hydrazinecarbonyl]benzamide]

Docking scores: 1XKK = -7.486

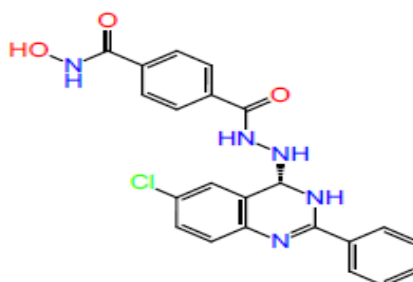
1T69 = -9.887



PV 59 [N-hydroxy-4-[N'-(7-methoxy-3,4-dihydroquinazolin-4-yl)hydrazinecarbonyl]benzamide]

Docking scores: 1XKK = -8.611

1T69 = -9.780



PV 60 [N-hydroxy-4-[N'-(6-chloro-2-phenyl-3,4-dihydroquinazolin-4-yl)hydrazinecarbonyl]benzamide]

Docking scores: 1XKK = -7.232

1T69 = -9.286

RESULTS AND DISCUSSION

From this data, it was found that by combining the pharmacophore of EGFR inhibitors and HDAC inhibitors, the new designed compound can inhibit both the targets with good binding affinity.

The compound EH01 showed 3H bond with Asp 800, ARG 811 and ASP 855 when docked against 1XKK. 3H bond with ASP 101, GLY 151 and GLY 206 and 2 pi-pi stacking with PHE 152 and PHE 208 with 1T69.

The compound EH02 showed 3H bond with ASP 100 and MET 793 when docked against 1XKK. 4 H bond with GLY 151 and ASP 101 and 1 pi-pi stacking with PHE 152 when docked with 1T69.

The compound EH03 showed 5H bond with CYS 797, ALA 722, ASP 837 and 855, ASN 942 with 1XKK. 2H bond with ASP 101 and GLY 151 and 2 pi-pi stacking with PHE 152 and 207 with 1T69.

Prediction of ADME Properties:

Poor pharmacokinetic profile is one of the major limitations for the failure of many drugs. Ideally drug should be easily absorbed from the site of administration, transported to active site without non-specific interactions, with maximum efficacy and safety, easily metabolized and eliminated without giving any toxic metabolites from the body are collectively termed as ADMET properties.

Predicting the ADMET properties by computational programs in the advanced stages of drug discovery helps in the design of safe and effective drugs; it also reduces cost and saves lot of time. ADMET related properties of the ligands were predicted by the Qikprop module of Schrodinger software.

According to Lipinski criteria for the drug candidate should have molecular weight ≤ 500 , $\log P \leq 5$, hydrogen bonding donors (HBD) ≤ 5 and hydrogen bonding acceptors (HBA) ≤ 10 . Most of the designed ligands obeyed Lipinski rules except PV25.

QPPCaco, QPlogBB represents the apparent cell permeability of the compounds. Caco-2 cell is best model and widely used to predict the apparent cell

RESULTS AND DISCUSSION

permeability of drug candidates for intestinal absorption. Recommended value by software is in the range of 25-500 i.e., less than 25 is poor and greater than 500 have high permeability.

Predictions are confined to non-active transport and all the ligands have QPPCaco value within the range except PV11, 12, 14, 18, 19, 21, 44, 56, 57. It reveals that ligands have good intestinal absorption.

QPlogBB values of the compounds are also found to be good except PV 11, 24, 25, 32, 44.

The aqua solubility parameter (QPlogS) of tested ligands were found in the permissible range (-6.5 to 0.5). However ligands PV11, 42, 45, 46, 47, 53, 54, 55 violate this rule.

Qikprop also explored the percent Human Oral Absorption of ligands most of the ligands had an excellent oral absorption. Those with good absorption are PV09, 20, 23, 41, 42, 43, 45, 46, 47, 49, 53, 54, 55, 58, 59, 60.

The estimation of surface contributions of polar fragments is determined by Topological Polar Surface Area (tPSA). All compounds had favourable tPSA values in the range of 51.91 to 127.87Å², which assures good impact on bioavailability of the molecule, except PV11.

The QPPMDCK predicted apparent MDCK cell permeability. MDCK cells are considered to be a good mimic for the blood–brain barrier. Higher the value of MDCK cell, higher the cell permeability. The results revealed that all the compounds were within range of limit except PV11, 14, 18, 19, 21, 24, 25, 32, 44, 56.

Based on the docking studies as well as pharmacokinetic studies three ligands have been selected for further screening. The selected ligands are PV58, 59 and 60. They were re-coded as EH01, EH02 and EH03 respectively for easy identification.

These selected compounds have entered into next phase of study.

Synthesis and Characterization:

RESULTS AND DISCUSSION

The selected compounds were synthesized using the above mentioned scheme and further analysis was done on those compounds.

The physical properties like melting point, solubility, and analytical studies like TLC, UV, IR and NMR spectroscopy of the synthesized compounds have been performed for identification of the compounds.

The NMR spectra for the prototype compound EH03 was found to be

15.03 (s, 1H - NH - OH)

12.52 (s, 1H - NH - OH)

11.5 (s, 1H NH - C = O)

10.5 (s, 1H Ar - NH)

8.71 - 7.41 (m, 13H, Ar - H)

The presence of these peaks showed the confirmation of the compound formation.

Biological activity:

***In-vitro* cytotoxicity studies:**

All the synthesized compounds were screened for their *in-vitro* cancer cell line assay based on cell viability using the dye 3-(4,5-dimethylthiazol-2-yl)-2,5-diphenyl tetrazolium bromide (MTT)

The microculture tetrazolium assay is based on metabolic reduction of dye MTT to water soluble blue formazan crystal by mitochondrial dehydrogenase enzyme.

The formation of formazan complex is directly proportional to number of viable cells. The compounds were tested against MCF-7 cell line.

All the compounds showed good inhibition of cell growth on screening. Their percentage inhibition was found to be 87.46, 76.64 and 86.96 for EH01, EH02 and EH03 respectively.

RESULTS AND DISCUSSION

The compound EH01 showed higher percentage inhibition of cell growth compared to others. The docking as well as pharmacokinetic properties of the Compound EH01 was also found to be good. Hence the development of compound EH01 and further screening of this compound can lead to identification of effective drug molecule.

CONCLUSION

A new series of quinazoline derivatives have been designed and evaluated *in-silico* for their activity as dual inhibitor against targets like EGFR and HDAC. The compounds with good efficacy and pharmacokinetics have been synthesized and screened for its efficacy *in-vitro*. The compound EH01 (N-hydroxy-4-[N'-(7-methoxy-2-phenyl-3,4-dihydroquinazolin-4-yl)hydrazinecarbonyl]benzamide) showed good anticancer activity against MCF-7 cell line. This opens an area on anticancer research by providing a small idea that by combining the pharmacophore of two different targets we can get a newer compound with greater efficacy towards both the targets.

BIBLIOGRAPHY

1. <https://www.who.int/en/news-room/fact-sheets/detail/cancer>
2. National Cancer Institute [Internet]. Available from: <https://www.cancer.gov/about-cancer/understanding/what-is-cancer>
3. <https://www.who.int/cancer/en/>
4. National Breast Cancer Foundation [Internet]. Available from: <https://www.nationalbreastcancer.org/what-is-breast-cancer>
5. Imran Ali, Waseem A. Wani and Kishwar Saleem. Cancer Scenario in India with Future Perspective. *J Cancer Ther.* 2011; 56-70.
6. Shreshtha Malvia, Sarangadhara Appalaraju Bagadi, Uma S. Dubey and Sunita Saxena. Epidemiology of breast cancer in Indian women. *Asia-Pac J Clin Oncol.* 2017; 1-6.
7. <https://www.cancer.net/cancer-types/breast-cancer/diagnosis>.
8. Dey, Sharma, Mishra, Krishnan, Govil, Dhillon. Breast Cancer Awareness and Prevention Behavior among Women of Delhi, India: Identifying Barriers to Early Detection. *Libert Academi.* 2016; 10:147-156.
9. Liao WS, Ho Y, Lin YW, Naveen Raj, Liu KK, Chen C, Zhou XZ, Lu KP, Chao JI. Targeting EGFR of triple-negative breast cancer enhances the therapeutic efficacy of paclitaxel- and cetuximab- conjugated nanodiamond nanocomposite. *Acta Biomater.* 2019 Mar 1; 86:395 - 405.
10. Joelle Roche, Philippe Bertrand. Inside HDACs with more selective HDAC inhibitors. *Eur J Med Chem.* 2016 Oct 4; 121:451-83.
11. Ahmed T. Negmeldin, Joseph R. Knoff, ary Kay H. Pflum. The structural requirements of histone deacetylase inhibitors: C4-modified SAHA analogs display dual HDAC6/HDAC8 selectivity. *Eur J Med Chem.* 2018; 143:1790-1806.
12. Li ED, Lin Q, Meng YQ, Zhang LY, Song PP, Li N, Xin JC, Yang P, Bao CN, Zhang DQ, Zhang Y, Wang JK, Zhang QR, Liu HM. 2, 4-Disubstituted quinazolines targeting breast cancer cells via EGFR-PI3K. *Eur J Med Chem.* 2019 Jun 15; 172: 36-47.
13. Melissa Oliveira-Cunha, William G. Newman, Ajith K. Siriwardena. Epidermal growth factor receptors in cancer. *Cancers.* 2011; 3: 1513-1526.

14. Richardo H. Alvarez, Vicente Valero and Gabriel N. Hortobagyi. Emerging targeted therapies for breast cancer. *J clin Onco.* 2010. Doi:10.1200/JCO.2009.21.8594
15. Xinyu Li, Chengzhe Wu, Xin Lin, Xuerong Cai, Linyi Liu, Guoshun Luo, Qidong You and Hua Xiang. Synthesis and biological evaluation of 3-aryl-quinolin derivatives as anti-breast cancer agents targeting ER α and VEGFR-2. *Eur J Med Chem.* 2019;161:445-455.
16. Miao Zuo, Yue-Wen Zheng, She-Min Lu, Yan Li, San-Qi Zhang. Synthesis and biological evaluation of N-aryl salicylamides with a hydroxamic acid moiety at 5-position as novel HDAC–EGFR dual inhibitors. *Bioorg. Med. Chem.* 2012; 20: 4405–4412 .
17. Bruna Zucchetti, Andrea Kazumi Shimada, Artur Katz, Giuseppe Curigliano. The role of Histone Deacetylase Inhibitors in Metastatic Breast Cancer. *The Breast.* 2018. doi: 10.1016/j.breast.2018.12.001
18. A. Gopi Reddy, V. Harinadha Babu, Y. Jaya Prakash Rao. A Review on Quinazolines as Anticancer Agents. *J Chem and Pharma.* 2017; 10 (3): 1492-1504.
19. Sui Xiong Cai, Nilantha Sirisoma, Azra Pervin, Hong Zhang, Songchun Jiang. Discovery of N-methyl-4-(4-methoxyanilino)quinazolines as potent apoptosis inducers. Structure–activity relationship of the *quinazoline* ring. *Bioorg and Med Chem L.* 2010; 20 (7): 2330 - 2334.
20. Chao Ding, Shaopeng Chen, Cunlong Zhang, Guangnan Hu, Wei Zhang, Lulu Li, Yu Zong Chen, Chunyan Tan, Yuyang Jiang. Synthesis and investigation of novel 6-(1,2,3-triazol-4-yl)-4-aminoquinazolin derivatives possessing hydroxamic acid moiety for cancer therapy. *Bioorg and Med Chem.* 2017; 251: 27-37.
21. Er-dongLi, QiaoLina, Meng, Lu-ye Zhang, Pan-pan Song, Na Li, Jing-chao Xin, Peng Yang, Chong-nan Bao, Dan-qing Zhang et al., 2,4-Disubstituted quinazolines targeting breast cancer cells via EGFR-PI3K. *Eur J Med Chem.* 2019; 172: 36 - 47.
22. Siavosh Mahboobi, Andreas Sellmer, Matthias Winkler, Emerich Eichhorn, Herwig Pongratz, Thomas Ciossek, Thomas Baer, Thomas Maier, and Thomas Beckers. Novel Chimeric Histone Deacetylase Inhibitors: A Series of Lapatinib Hybrides as Potent Inhibitors of Epidermal Growth Factor Receptor (EGFR),

- Human Epidermal Growth Factor Receptor 2 (HER2), and Histone Deacetylase Activity. *J Med Chem.* 2010; 53:8546 - 8555.
23. Weiwei Yu, Weiqiang Lu, Guoliang Chen, Feixiong Cheng, Hui Su, Yihua Chen, Mingyao Liu, Xiufeng Pang. Inhibition of Histone Deacetylases Sensitizes EGFR-TKI-Resistant Non-Small Cell Lung Cancer Cells to Erlotinib *In Vitro* and *In Vivo*. *Br J Pharmacol.* 2017 Oct; 174(20): 3608-3622.
24. Y.-C. Duan, Y.-C. Ma, W.-P. Qin, L.-N. Ding, Y.-C. Zheng, Y.-L. Zhu, X.-Y. Zhai, J. Yang, C.-Y. Ma, Y.-Y. Guan. Design and synthesis of tranlycypromine derivatives as novel LSD1/HDACs dual inhibitors for cancer treatment. *Eur J Med Chem.* 2017. doi:10.1016/j.ejmech.2017.09.038.
25. B. Sever, M.D. Altıntop, M.O. Radwan, A. Özdemir, M. Otsuka, M. Fujita, H.I.Ciftci. Design, synthesis and biological evaluation of a new series of thiazolyl-pyrazolines as EGFR and HER2 inhibitors. *Eur J Med Chem.* 2019.
26. M. Huang, J. Zhang, C. Yan, X. Li, J. Zhang, R. Ling. Small molecule HDAC inhibitors: promising agents for breast cancer treatment. *Bioorg Chem.* 2019.
27. F.-W. Peng, J. Xuan, T.-T. Wu, J.-Y. Xue, Z.-W. Ren, D.-K. Liu, X.-Q. Wang, X.-H. Chen, J.-W. Zhang, Y.-G. Xu, L. Shi. Design, synthesis and biological evaluation of Nphenylquinazolin-4-amine hybrids as dual inhibitors of VEGFR-2 and HDAC. *Eur J Med Chem.* 2016. doi: 10.1016/j.ejmech.2015.12.033.
28. Laura Taddiaa, Domenico D'Arcab, Stefania Ferrara, Chiara Marraccinia, Leda Severia, Glauco Ponterinia, Yahuda G. Assarafc, Gaetano Marvertib, Maria Paola Costi. Inside the biochemical pathways of thymidylate synthase perturbed by anticancer drugs: Novel strategies to overcome cancerchemoresistance. *Drug Resistance Updates.* 2015; 23: 20–54.
29. Krishnan Suresh Kumar, Swastika Ganguly, Ravichandran Veerasamy, Erik De Clercq. Synthesis, antiviral activity and cytotoxicity evaluation of Schiff bases of some 2-phenyl quinazoline-4(3)H-ones. *Eur J Med Chem.* 2010; 45: 5474 -79.
30. Adel S. El-Azab, Mohamed A. Al-Omar, Alaa A.-M. Abdel-Aziz, Naglaa I. Abdel-Aziz, Magda A.-A. El-Sayed, Abdulaziz M. Aleisa, Mohamed M. Sayed-Ahmed, Sami G. Abdel-Hamide. Design, synthesis and biological evaluation of novel quinazoline derivatives as potential antitumor agents: Molecular docking study. *Eur J Med Chem.* 2010; 45: 4188-4198.

31. Mukesh B, Rakesh Kumar. Molecular Docking: A review. *International Journal of Research in Ayurveda and Pharmacy*. 2011; 2(6): 1746-1751.
32. M. Gnana Ruba Priya Girija K, Ravichandran N. In vitro study of anti-inflammatory and antioxidant activity of 4-(3h)-quinazolinone derivatives. *Ras Journal of chemistry*, 2011; 4: 410 - 418.
33. Ch.Rajver, Ch.Swarnalatha, B.Stephen Rathinaraj, S.Sudharshini. Synthesis of 6-bromo-oxo quinazoline derivatives and their Pharmacological activities, *Int J Chem Research*. 2010; 1 (1): 21-24.
34. Adel S. El-Azab, Mohamed A. Al-Omar, Alaa A.-M. Abdel-Aziz, Naglaa I. Abdel-Aziz, Magda A.-A. El-Sayed, Abdulaziz M. Aleisa, Mohamed M. Sayed-Ahmed, Sami G. Abdel-Hamide. Design, synthesis and biological evaluation of novel quinazoline derivatives as potential antitumor agents:Molecular docking study. *Eur j Med Chem*. 2010; 45: 4188-4198.
35. Sandip S. Kotgire, S. H. Mahajan, S. V. Amrutkar, U. D. Bhagat. Synthesis of ethyl 2-(2-methyl-4-oxoquinazolin-3(4H)-yl) acetate as important analog and intermediate of 2,3 disubstituted quinazolinones. *J. Pharm. Sci. & Res*. 2010; 2 (8): 518-520.
36. AAF. Wasfy, NA. Mohamed and AA. Salman. Synthesis and anti-cancer properties of novel quinazoline derivatives. *IJRPC*. 2015; 5 (1): 34-40.
37. Yaling Zhang, Qiaoli Hou, Xiabing Li, Jiuling Zhu, Wei Wang, Baolin Li, Lijun Zhao, Haibin Xia. Enrichment of novel quinazoline derivatives with high antitumor activity in mitochondria tracked by its self-fluorescence. *Eur J Med Chem*. 2019; 178: 417 -432.
38. Kapil Juvale, Jennifer Gallus, Michael Wiese. Investigation of quinazolines as inhibitors of breast cancer resistance protein (ABCG2). *Bioorg Med Chem*. 2013; 21: 7858-7873.
39. Zhuang Yang, Mingsheng Shen, Minghai Tang, Wanhua Zhang *et al.*, Discovery of 1,2,4-oxadiazole-Containing hydroxamic acid derivatives as histone deacetylase inhibitors potential application in cancer therapy. *Eur J Med Chem*. 2019; 178: 116-130.
40. Alshimaa M.A. Aboeldahab, Eman A.M. Beshr, Mai E. Shoman, Safwat M. Rabea, Omar M. Aly. Spirohydantoin and 1,2,4-triazole-3-carboxamide

- derivatives as inhibitors of histone deacetylase: Design, synthesis, and biological evaluation. *Eur J Med Chem.* 2018; 146: 79-92.
41. Mosmann, T. et.al., Rapid colorimetric assay for cellular growth and survival: application to proliferation and cytotoxicity assays. *J Immun Methods.* 1983; 65: 55-63.
42. Monks, A., Scudiero, D., Skehan, P., Shoemaker, R., Paull, K., Vistica, D., Hose, C., Langley, J., Cronise, P., Vaigro-Wolff, A., Gray-Goodrich, M., Campbell, H., Mayo, J., Boyd. Feasibility of high flux anticancer drug screen using a diverse panel of cultured human tumour cell lines. *Journal of the National Cancer Institute.* 1991; 83: 757-766.